Technical Memorandum ERL WPL-188

APERTURE-AVERAGING FACTOR FOR OPTICAL PROPAGATION THROUGH THE TURBULENT ATMOSPHERE

James H. Churnside

Wave Propagation Laboratory
Boulder, Colorado
November 1990

noaa NATIONAL OCEANIC AND ATMOSPHERIC ADMINISTRATION / Environmental Research Laboratories

NOAA Technical Memorandum ERL WPL-188

APERTURE-AVERAGING FACTOR FOR OPTICAL PROPAGATION THROUGH THE TURBULENT ATMOSPHERE

James H. Churnside

Wave Propagation Laboratory
Boulder, Colorado
November 1990

UNITED STATES
DEPARTMENT OF COMMERCE

Robert A. Mosbacher
Secretary

NATIONAL OCEANIC AND
ATMOSPHERIC ADMINISTRATION

John A. Knauss
Under Secretary for Oceans
and Atmosphere/Administrator

Environmental Research
Laboratories

Joseph O. Fletcher
Director

NOTICE

Mention of a commercial company or product does not constitute an endorsement by NOAA/ERL. Use of information from this publication concerning proprietary products or the tests of such products for publicity or advertising purposes is not authorized.

For sale by the National Technical Information Service, 5285 Port Royal Road
Springfield, VA 22161

CONTENTS

Abstract. We have developed approximate expressions for the aperture-averaging factor of optical scintillation in the turbulent atmosphere. For large apertures and weak path-integrated turbulence with small inner scale, the variance of signal fluctuations is proportional to the –7/3 power of the ratio of the aperture diameter to the Fresnel zone size. If the inner scale is large, the variance is proportional to the –7/3 power of the ratio of the aperture diameter to the inner scale. In strong, path-integrated turbulence, two scales develop. That portion of the variance associated with the smaller scale is proportional to the –2 power of the ratio of the aperture diameter to the phase coherence length. That portion of the variance associated with the larger scale is proportional to the –7/3 power of the ratio of the aperture diameter to the scattering disk. These simple approximations are within a factor of 2 of the measurements. The probability density function is nearly log normal under most conditions.

1. INTRODUCTION

As light propagates through the atmosphere, it is randomly scattered by refractive turbulence inhomogeneities. At some distance from the source, an irradiance pattern is produced that is random in both space and time. An optical receiver with a very small aperture will produce a random signal. If the aperture is larger than the spatial scale of the irradiance fluctuations, the receiver will average fluctuations over the aperture, and the signal fluctuations will be less than those from a point receiver. We define the aperture-averaging factor A as the ratio of the signal fluctuations from a receiver with aperture diameter D to those from a receiver with an infinitesimally small aperture.

Fried,[1] following a development by Tatarskii,[2] presented a formula for the aperture-averaging factor in the general case. This same formula was also derived in Refs. 3–5. Fried concluded that the averaging factor is proportional to the inverse square of aperture diameter for large apertures in weak turbulence. This conclusion was based on incorrect numerical calculations, and the correct –7/3 power dependence was obtained.[6] Note that the inverse square law was also obtained,[4] based on an incorrect form for the irradiance covariance function. Approximations for the weak turbulence case were given for several geometries.[7–10]

Early experiments compared measured aperture-averaging factors with the weak-turbulence theory and found very poor agreement.[11,12] At the time, the phenomenon of saturation of scintillation was not understood, and these results were probably not in the weak-turbulence regime. Later experiments that were clearly in the weak-turbulence regime showed much better agreement.[13,14]

No good theory exists for the strong-turbulence regime. Gracheva and Gurvich[3] used measured covariance functions to obtain numerical estimates of the aperture-averaging factor for those cases. They concluded that there was generally less aperture averaging in strong turbulence than one would expect from the weak-turbulence theory. This is in qualitative agreement with the results of Refs. 11 and 12. A later series of measurements, intentionally made in strong turbulence, also showed less aperture averaging in strong turbulence.[15]

In this report we first review the theory for aperture averaging in weak turbulence. The theory for large values of the inner scale of turbulence, which has not been reported in the literature, is also included. We then develop the theory for strong turbulence using asymptotic formulas of the covariance function. In all cases, the emphasis is on simple approximations rather than extremely precise, multiple-integral expressions. These formulas are then compared with experimental results.

2. THEORY

The general form of the aperture-averaging factor for a circular aperture of diameter D is[1]

$$A = \frac{16}{\pi D^2} \int_0^D \frac{C_I(\varrho)}{C_I(0)} \left[\cos^{-1}\left(\frac{\varrho}{D}\right) - \frac{\varrho}{D}\left(1 - \frac{\varrho^2}{D^2}\right)^{1/2} \right] \varrho d\varrho \ , \tag{1}$$

where $C_I(\varrho)$ is the covariance function of irradiance, $C_I(0)$ is the variance of irradiance, and the quantity within the square brackets is the area of overlap of two circles of diameter D whose centers are located a distance ϱ apart. A simple change of variable yields an equation that is simpler to work with,

$$A = \frac{16}{\pi} \int_0^1 \frac{C_I(Dy)}{C_I(0)} [\cos^{-1} y - y(1-y^2)^{1/2}] y dy \ . \tag{2}$$

2.1 Weak Turbulence

We define weak turbulence as the condition when the transverse coherence length of the field in the receiver plane is much larger than the Fresnel zone size. Under these conditions, the standard deviation of the irradiance fluctuations will be much less than the mean irradiance, and the fluctuations will have a lognormal distribution. The covariance function is given by.[16]

$$C_I(\varrho) = 16\pi^2 k^2 \int_0^\infty dK \, K \Phi_n(K) \int_0^L dz \, J_0(K\varrho s) \, \sin^2\left[\frac{K^2(L-z)s}{2k}\right] , \tag{3}$$

where k is the optical wavenumber, $\Phi_n(K)$ is the spectrum of refractive index fluctuations, L is path length, J_0 is the zero-order Bessel function of the first kind, and s is a geometry factor that is unity for a plane wave and z/L for a spherical wave. In Eq. (3), isotropic, homogeneous turbulence is implicitly assumed. The case where turbulence strength is a slowly varying function of position will also be discussed.

2.1.1 Plane wave, small inner scale

For plane-wave propagation, $s = 1$. For a very small value of the inner scale of turbulence, $[\ell_0 << (L/k)^{1/2}]$, we can use the Kolmogorov spectrum[16]

$$\Phi_n(K) = 0.033 \, C_n^2 \, K^{-11/3} \ , \tag{4}$$

where C_n^2 is the refractive turbulence structure parameter. These two conditions imply

$$C_I(\varrho) = (0.033)16\pi^2 k^2 C_n^2 \int_0^\infty dK \, K^{-8/3} \int_0^L dz \, J_0(K\varrho) \ \sin^2\left[\frac{K^2(L-z)}{2k}\right] . \tag{5}$$

If we let $\varrho = 0$, we can easily evaluate the integrals to obtain

$$C_I(0) = 1.23 \, k^{7/6} \, L^{11/6} \, C_n^2 \ . \tag{6}$$

The aperture-averaging factor is therefore

$$A = 21.6\, k^{5/6}\, L^{-11/6} \int_0^\infty dK\, K^{-8/3} \int_0^L dz\, \sin^2\left[\frac{K^2(L-z)}{2k}\right] \times \int_0^1 dy\, y\, J_0(KDy)[\cos^{-1} y - y(1-y^2)^{1/2}] \,. \tag{7}$$

We note that the y integral is given by $\pi\, J_1^2(KD/2)/K^2D^2$ and let $u = KD/2$. After some manipulation we obtain

$$A = 8.47\left(\frac{kD^2}{4L}\right)^{5/6} \int_0^\infty du\, u^{-14/3}\, J_1^2(u)\left[1 - \frac{kD^2}{4Lu^2}\sin\left(\frac{4Lu^2}{kD^2}\right)\right], \tag{8}$$

which is a function only of $(kD^2/4L)^{1/2}$, the ratio of the aperture radius $D/2$ to the Fresnel zone size $(L/k)^{1/2}$. This function is plotted as a solid line in Fig. 1.

If we let $v = 4Lu^2/kD^2$, we can rewrite Eq. (8) as

$$A = 4.24\frac{4L}{kD^2} \int_0^\infty dv\, v^{-17/6}\left(1 - \frac{\sin v}{v}\right) J_1^2\left[\left(\frac{kD^2 v}{4L}\right)^{1/2}\right]. \tag{9}$$

For small aperture diameter ($kD^2/4L << 1$), we note that $J_1(a) \approx \frac{1}{2}\, a$ over most of the integration range of interest. We can then perform the integral in Eq. (9) to get $A = 1$ for small apertures. This, of course, is what we would expect.

For a large aperture ($kD^2/4L >> 1$), we note that the argument of the sine function in Eq. (8) will generally be small. Therefore, we note that $\sin a \approx a - a^3/6$ for small a and

$$A \approx 1.41\left(\frac{kD^2}{4L}\right)^{-7/6} \int_0^\infty du\, u^{-2/3}\, J_1^2(u) = 0.932\left(\frac{kD^2}{4L}\right)^{-7/6}. \tag{10}$$

Note that the variance decreases faster than D^{-2} with increasing aperture size. A D^{-2} dependence is what one would expect for a collection of perfectly coherent areas on the detector that are mutually independent. The faster $D^{-7/3}$ dependence is due to the small angle of turbulent scattering. Light propagating toward the center of the receiver is unlikely to be scattered by an angle large enough to miss the receiver entirely. This implies that the correlation function of irradiance fluctuations goes negative at some separation, since areas near the center are likely to be brighter than average when the center is darker, and vice versa. To generalize, it seems a correlation function that goes negative can produce an aperture-averaging factor that falls off faster than D^{-2} for large apertures.

Following previous authors,[6, 9, 14] we use the interpolation formula

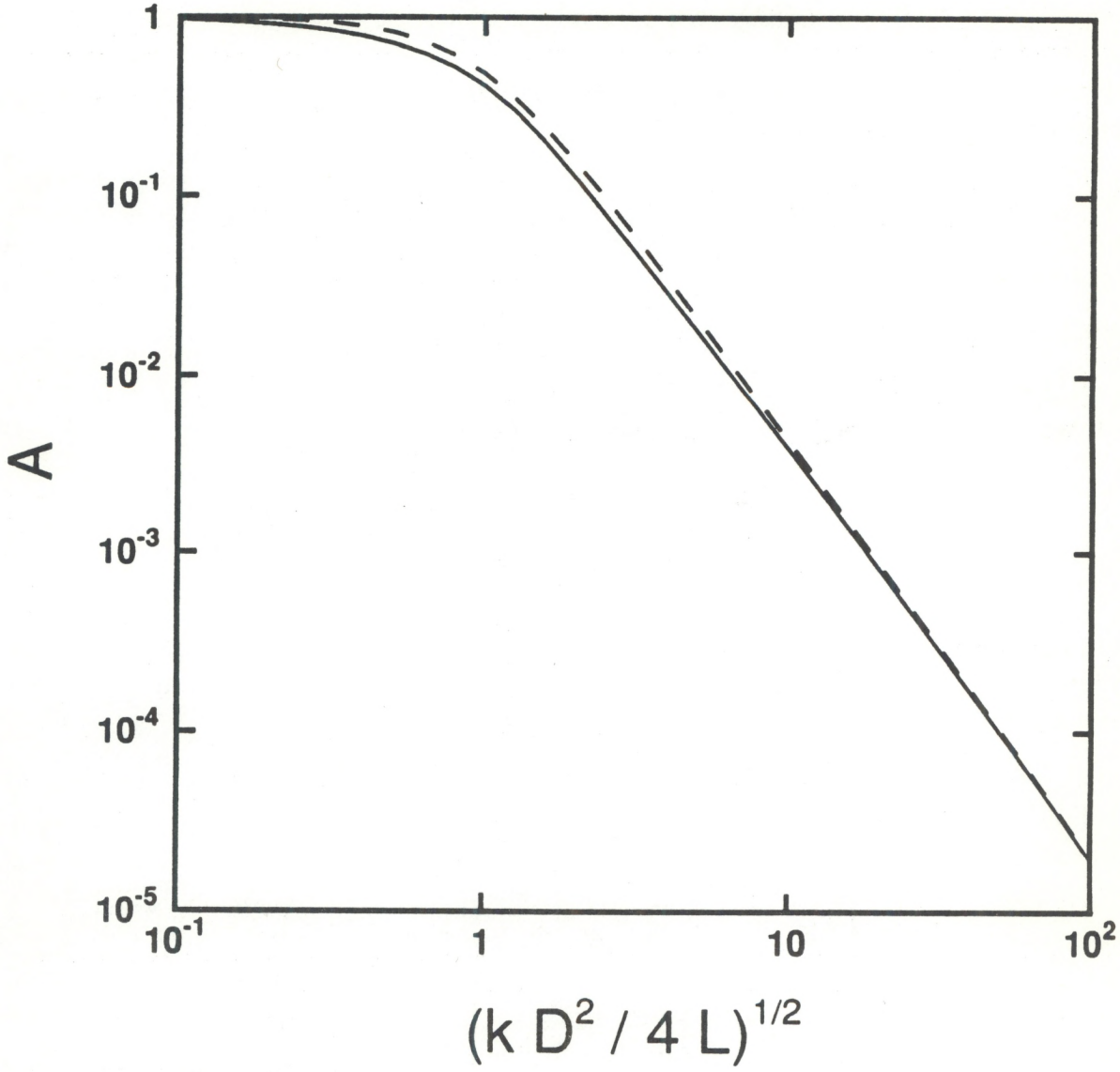

Figure 1. Aperture-averaging factor A vs. ratio of aperture radius $D/2$ to Fresnel zone size $(L/k)^{1/2}$ for plane-wave propagation through weak turbulence with small inner scale. The solid line is the exact formula, and the dashed line is the recommended approximation.

$$A = \left[1 + 1.07\left(\frac{kD^2}{4L}\right)^{7/6}\right]^{-1} . \tag{11}$$

This function is plotted as a dashed line in Fig. 1. The agreement is generally very good, although the approximation of Eq. (11) is somewhat lower than the exact formula of Eq. (8) for $kD^2/4L$ values near unity (17% low at 1). Fried[6] has attempted to improve the fit in this area with an additional $(kD^2/4L)^{7/12}$ term that was fitted empirically. However, this is difficult to generalize and we prefer Eq. (11) despite its shortcomings.

If turbulence is not homogeneous, Eq. (11) needs to be modified. We assume that C_n^2 is a function of position z along the path, but that it is nearly constant over distances less than the aperture diameter in any direction perpendicular to propagation (e.g., across the beam). In this case, we can replace C_n^2 in Eq. (5) by $C_n^2(z)$, which must be moved into the z integral. From there we see that

$$C_I^2(0) = 1.23\ k^{7/6}\ L^{11/6}\ \frac{11}{6}\int_0^1 dx(1-x)^{5/6}\ C_n^2(xL) . \tag{12}$$

It is also straightforward to show that

$$A = \left[1 + 1.07\ C\left(\frac{kD^2}{4L}\right)^{7/6}\right]^{-1} , \tag{13}$$

where

$$C = \frac{11\int_0^1 dx(1-x)^{5/6}\ C_n^2(xL)}{18\int_0^1 dx(1-x)^2\ C_n^2(xL)} . \tag{14}$$

where $C_n^2(L)$ is the turbulence strength at the receiver.

2.1.2 Plane wave, large inner scale

For very large inner scale [$\ell_0 >> (L/k)^{1/2}$], we can use the Tatarskii spectrum[16]

$$\Phi_n(K) = 0.033\ C_n^2\ K^{-11/3} \exp(-0.0285\ K^2\ell_0^2) . \tag{15}$$

This implies that

$$C_I(\varrho) = (0.033)16\pi^2\ k^2\ C_n^2 \int_0^\infty dK\ K^{-8/3} \exp(-0.0285\ K^2\ \ell_0^2) \tag{16}$$

$$\times \int_0^L dz\ J_0(K\varrho)\ \sin^2\left[\frac{K^2(L-z)}{2k}\right] .$$

We note that the argument of the sine function will be small over most of the range of the integral so that we can let the sine equal its argument. This allows the z integral to be evaluated, with the result

$$C_I(\varrho) = (0.033)\frac{4}{3}\pi^2 L^3 C_n^2 \int_0^\infty dK\, K^{4/3} J_0(K\varrho)\exp(-0.0285K^2\ell_0^2) . \tag{17}$$

Letting $\varrho \to 0$, we have

$$C_I(0) = 12.8\, L^3\, C_n^2\, \ell_0^{-7/3} .$$

The aperture-averaging factor is

$$A = 0.686\left(\frac{D}{\ell_0}\right)^{-7/3} \int_0^\infty du\, u^{-2/3}\, J_1^2(u) \exp\left(-0.1141\frac{\ell_0^2\, u^2}{D^2}\right) . \tag{18}$$

This is plotted as a function of D/ℓ_0 as a solid line in Fig. 2. Note that as D gets very large the exponential in Eq. (18) goes to unity, and the integral can be evaluated to get

$$A = 0.453\left(\frac{D}{\ell_0}\right)^{-7/3} . \tag{19}$$

This leads to the approximate formula

$$A = \left[1 + 2.21\left(\frac{D}{\ell_0}\right)^{7/3}\right]^{-1} . \tag{20}$$

This is plotted as a dashed line in Fig. 2. As in Fig. 1, Fig. 2 shows fairly good agreement between the exact and the approximate formulas. The worst agreement is near $D/\ell_0 = 1$, with an error of about 34% at that point. This is somewhat worse than the small-inner-scale case.

The Tatarskii spectrum was used in the above calculations because of its simplicity. Actually, the more rigorous Hill spectrum[17, 18] should be used. It can be approximated by[19]

$$\begin{aligned}\Phi_n(K) = 0.033\, C_n^2\, K^{-11/3}\, \{ &\exp(-1.29\, K^2\, \ell_0^2) \\ &+ 1.45\, \exp[-0.97\, (\ln K\, \ell_0 - 0.452)^2]\} .\end{aligned} \tag{21}$$

The aperture-averaging factor was recalculated for this case using the approximate Hill spectrum. The numerical results are plotted as discrete points in Fig. 2. We see that the Tatarskii spectrum results are very close to the Hill spectrum results. Where the largest discrepancies exist, near D/ℓ_0, our approximate formula for A of Eq. (20) is closer to the more-precise Hill spectrum values than to the Tatarskii spectrum values. Hence, we feel justified in using the Tatarskii spectrum to develop Eq. (20).

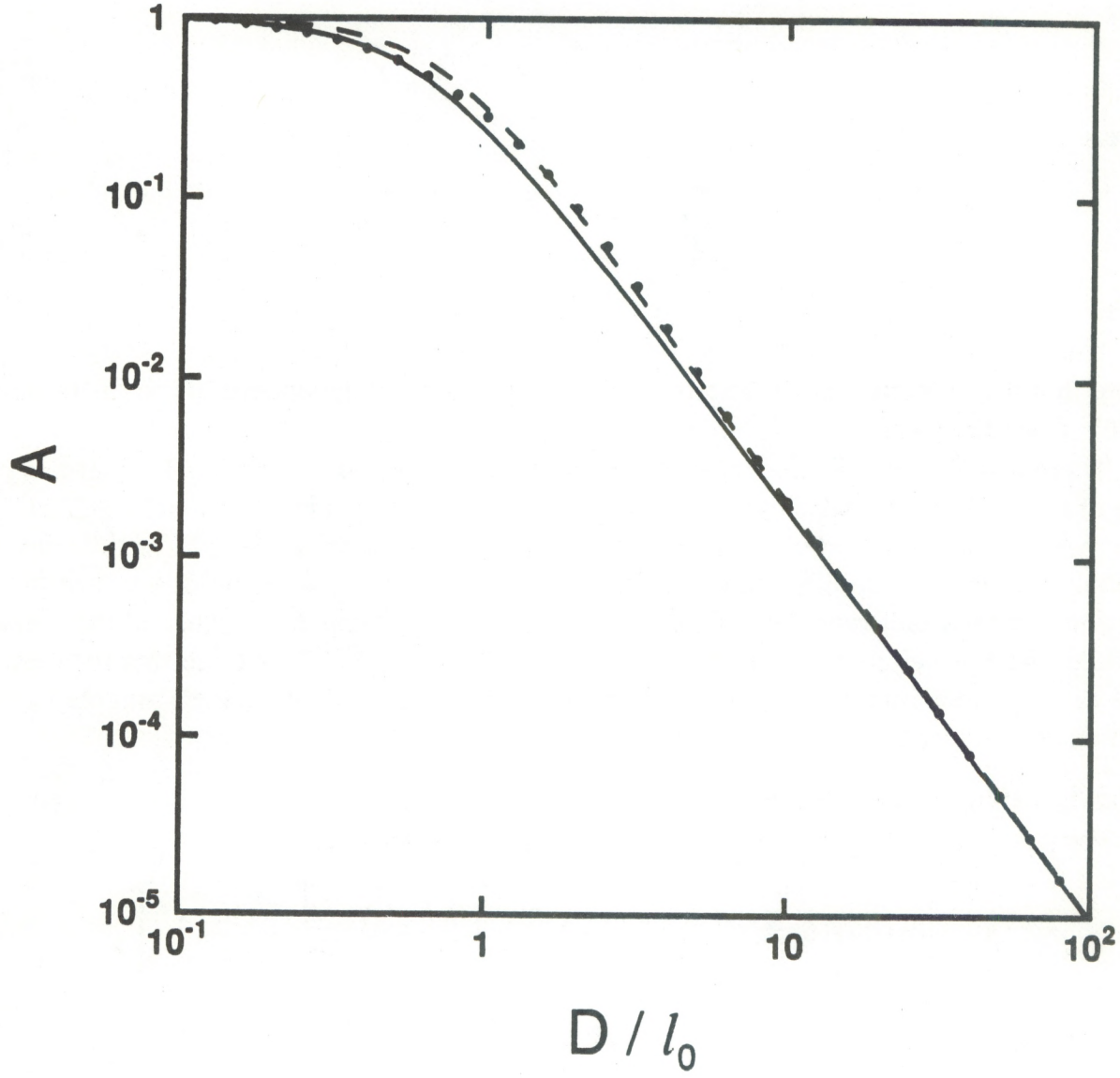

Figure 2. Aperture-averaging factor A vs. ratio of aperture diameter D to inner scale ℓ_0 for plane-wave propagation through weak turbulence with large inner scale. The solid line is the exact formula using the Tatarskii spectrum, the points are exact values using the Hill spectrum, and the dashed line is the recommended approximation.

We can also evaluate the case where C_n^2 and ℓ_0 are functions of path position. It is straightforward to show that this leads to

$$C_I(0) = 38.3\ L^3 \int_0^1 dx(1-x)^2\ C_n^2(xL)\ \ell_0^{-7/3}(xL)\ , \tag{22}$$

and

$$A \approx [1 + 2.21\ C\ D^{7/3}]^{-1}\ , \tag{23}$$

where

$$C = \frac{\int_0^1 dx(1-x)^2\ C_n^2(xL)\ \ell_0^{-7/3}(xL)}{\int_0^1 dx(1-x)^2\ C_n^2(xL)}\ . \tag{24}$$

Note that if ℓ_0 is constant, the aperture-averaging factor is independent of the distribution of C_n^2 along the path.

There remains the question of what to do when the inner scale and the Fresnel zone are of the same order. We note that Eqs. (11) and (20) are equal when $\ell_0 = 2.73(L/k)^{1/2}$. We therefore recommend using the small-inner-scale result when $\ell_0 < 2.73(L/k)^{1/2}$ and the large-inner-scale results when $\ell_0 > 2.73(L/k)^{1/2}$. In Fig. 3, we plotted this approximation and the exact values using the Hill spectrum as functions of the ratio of the inner scale to the Fresnel zone for $D/\ell_0 = 10$ and for $(kD^2/4L)^{1/2} = 10$. We see that for these two cases there is reasonable agreement between the simple approximation and the exact values.

2.1.3 Spherical wave, small inner scale

For spherical wave propagation, $s = z/L$. For small inner scale,

$$C_I(\varrho) = (0.033)16\pi^2k^2C_n^2 \int_0^\infty dK\ K^{-8/3} \int_0^L dz\ J_0\left(\frac{K\varrho z}{L}\right)\sin^2\left[\frac{K^2z(L-z)}{2kL}\right]\ . \tag{25}$$

Letting $\varrho = 0$ produces

$$C_I(0) = 0.497\ k^{7/6}\ L^{11/6}\ C_n^2\ . \tag{26}$$

The aperture-averaging factor is

$$\begin{aligned} A = {} & 53.4\ k^{5/6}\ L^{-11/6} \int_0^\infty dK\ K^{-8/3} \int_0^L dz\ \sin^2\left[\frac{K^2z(L-z)}{2kL}\right] \\ & \times \int_0^1 dy\ y\ J_0\left(\frac{KDzy}{L}\right)[\cos^{-1} y - y(1-y^2)^{1/2}]\ . \end{aligned} \tag{27}$$

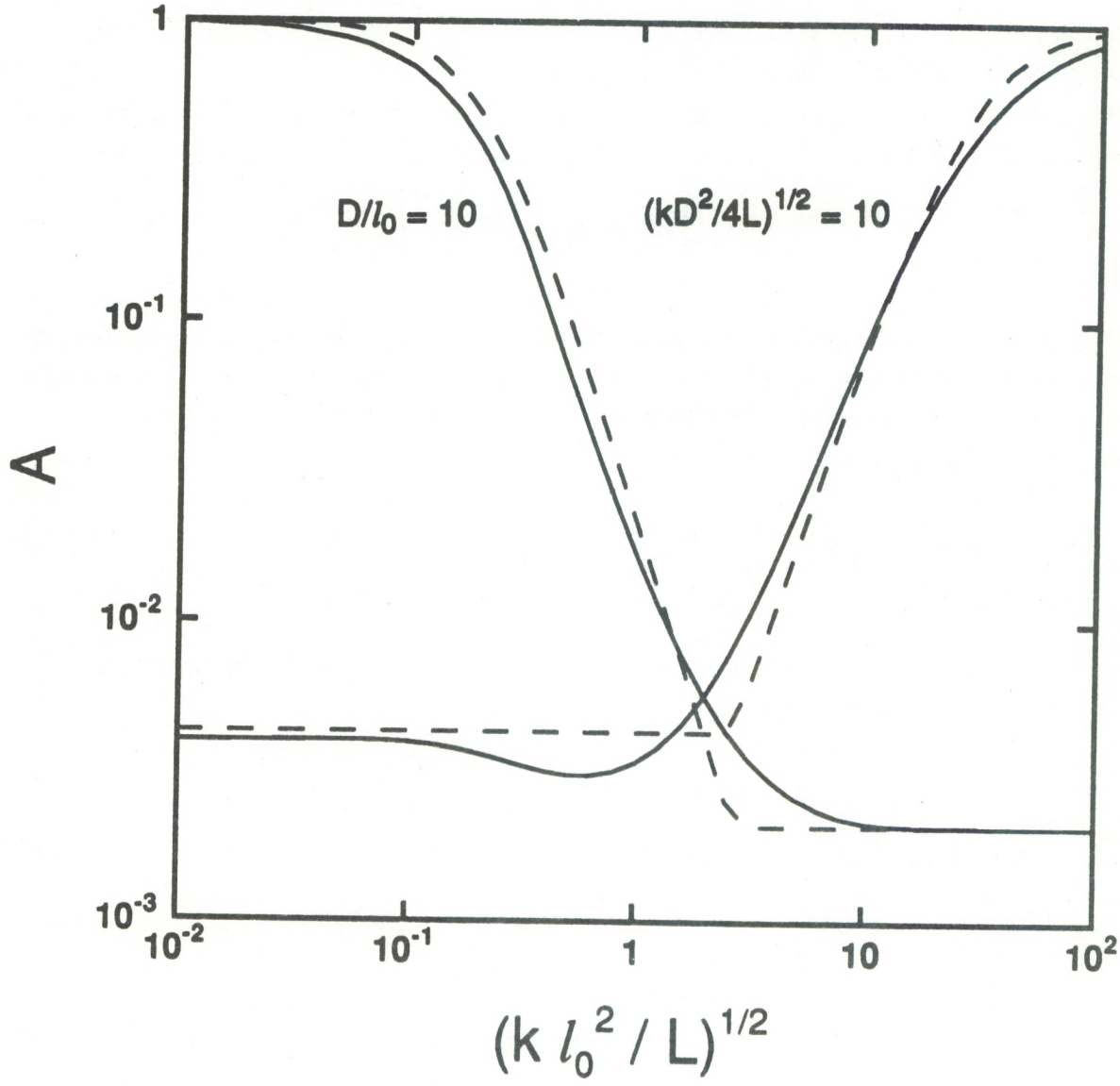

Figure 3. Aperture-averaging factor A vs. ratio of inner scale ℓ_0 to Fresnel zone size $(L/K)^{1/2}$ for plane-wave propagation with aperture size as labeled. The solid lines are the exact formula using the Hill spectrum, and the dashed lines are the approximate values.

We can evaluate the y-integral as before. We also let $u = DzK/2L$ and $x = z/L$. After some manipulation,

$$A = 41.9\left(\frac{kD^2}{4L}\right)^{5/6}\int_0^\infty du\; u^{-14/3}\, J_1^2(u)\int_0^1 dx\; x^{5/3}\,\sin^2\left[\frac{1}{2}\frac{4L}{kD^2}\left(\frac{1}{x}-1\right)u^2\right]. \tag{28}$$

This is plotted as the solid line in Fig. 4.

For large D, the sine function can be replaced by its argument and the integrals can be evaluated analytically. This leads to the approximation

$$A = \left[1 + 0.214\left(\frac{kD^2}{4L}\right)^{7/6}\right]^{-1}, \tag{29}$$

which is plotted as a dashed line in Fig. 3. Once again we see reasonable agreement, although not as good as for the plane-wave case for $D/2$ near $(k/L)^{1/2}$. At $D/2$ equal to two Fresnel zones, the approximation is nearly a factor of 2 (86%) high.

For inhomogeneous turbulence,

$$C_I^2(0) = 0.497k^{7/6}\,L^{11/6}\frac{\Gamma\left(\frac{11}{3}\right)}{\Gamma^2\left(\frac{11}{6}\right)}\int_0^1 dx\; x^{5/6}\,(1-x)^{5/6}C_n^2(xL)\,, \tag{30}$$

where Γ is the gamma function. The ratio $\Gamma(11/3)/\Gamma^2(11/6) = 4.53$. The aperture-averaging function is given by

$$A = \left[1 + 0.214\; C\left(\frac{kD^2}{4L}\right)^{7/6}\right]^{-1}, \tag{31}$$

where

$$C = \frac{2\Gamma\left(\frac{2}{3}\right)\int_0^1 dx\; x^{5/6}(1-x)^{5/6}\; C_n^2(xL)}{\Gamma^2\left(\frac{11}{6}\right)\int_0^1 dx\; x^{-1/3}(1-x)^2\; C_n^2(xL)}\,. \tag{32}$$

In this equation, $2\Gamma(2/3)/\Gamma^2(11/6) = 3.06$.

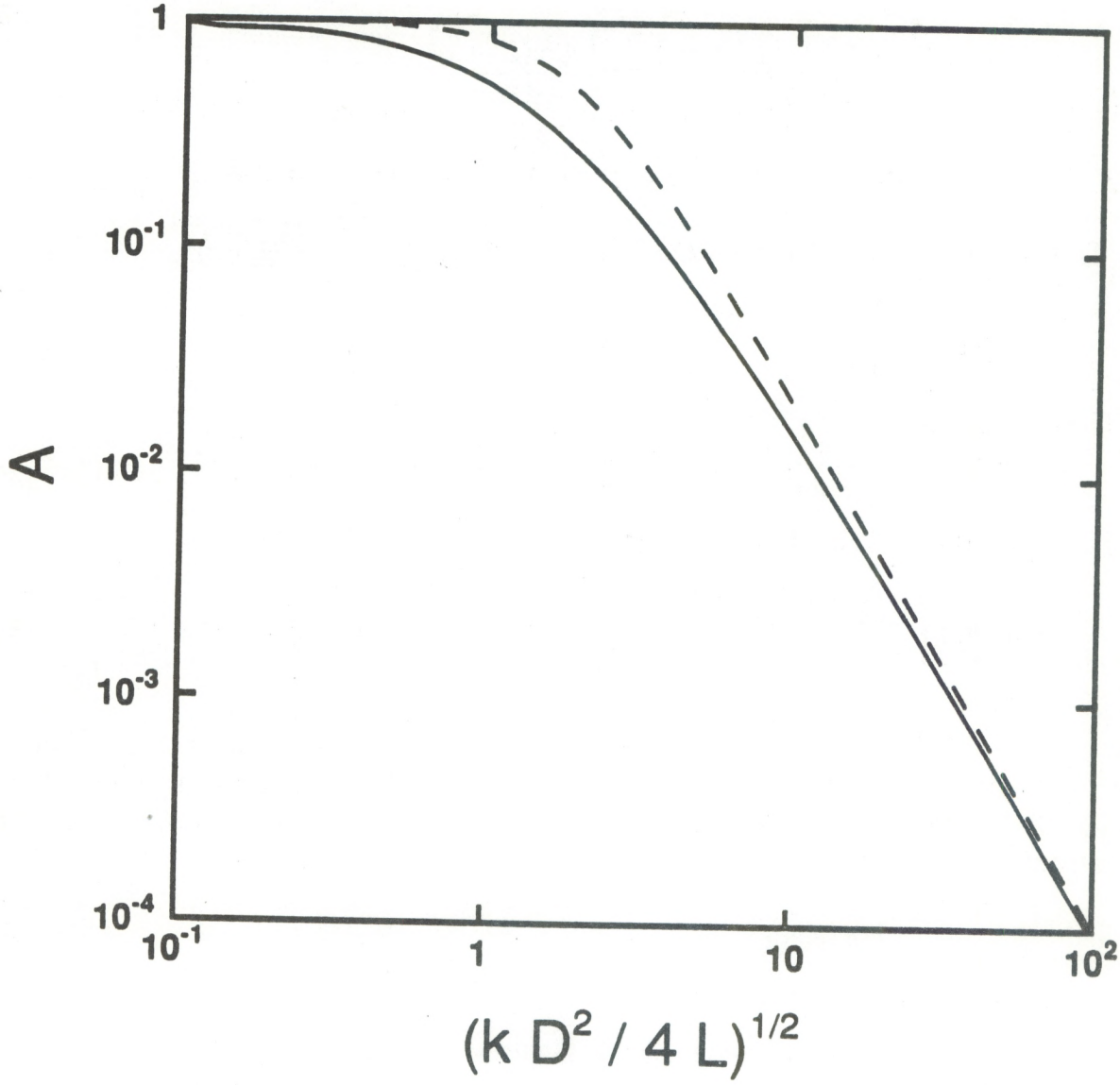

Figure 4. Aperture-averaging factor A vs. ratio of aperture radius $D/2$ to Fresnel zone size $(L/K)^{1/2}$ for spherical-wave propagation through weak turbulence with small inner scale. The solid line is the exact formula, and the dashed line is the recommended approximation.

2.1.4 Spherical wave, large inner scale

For the Tatarskii spectrum,

$$C_I(\varrho) = (0.033)16\pi^2\, k^2\, C_n^2 \int_0^\infty dK\, K^{-8/3}\exp(-0.0285K^2\ell_0^2) \times \int_0^L dz\, J_0\left(\frac{K\varrho z}{L}\right)\sin^2\left[\frac{K^2 z(L-z)}{2kL}\right] . \tag{33}$$

Here also, we can approximate the sine function by its argument so that

$$C_I(\varrho) = (0.033)4\pi^2\, C_n^2\, L^{-2}\int_0^\infty dK\, K^{4/3}\exp(-0.0285K^2\ell_0^2)\int_0^L dz\, z^2(L-z)^2 \times J_0\left(\frac{K\varrho z}{L}\right) . \tag{34}$$

The variance is

$$C_I(0) = 1.28\, L^3\, C_n^2\, \ell_o^{-7/3} \quad . \tag{35}$$

The aperture-averaging function is

$$A = 20.6\left(\frac{D}{\ell_0}\right)^{-7/3}\int_0^\infty du\, u^{-2/3}J_1^2(u)\int_0^1 dx\, x^{-1/3}(1-x)^2\exp\left(-0.114\frac{\ell_0^2u^2}{D^2x^2}\right) , \tag{36}$$

where $u = z\,D\,k/2L$ and $x = z/L$. This function is plotted as a solid line in Fig. 5. For large D/ℓ_0, the exponential in Eq. (36) is nearly unity and the remaining integrals can be evaluated. As before, this leads to an approximation for the aperture averaging, given in this case by

$$A = \left[1 + 0.109\left(\frac{D}{\ell_0}\right)^{7/3}\right]^{-1} , \tag{37}$$

which is plotted as the dashed line in Fig. 5. Again we see that the approximate formula is not as good for spherical-wave propagation as it is for plane-wave propagation, especially near the shoulder of the curve. In this case, the approximation is slightly more than a factor of 2 (118%) too high for $D/2 = \ell_0$.

The exact values were also calculated using the Hill spectrum. No significant difference between the Tatarskii-spectrum values and the Hill-spectrum values was observed, and these points are not in the figure.

For nonhomogeneous turbulence, it is straightforward to show that

$$C_I(0) = 38.3\, L^3\int_0^1 dx\, x^2\,(1-x)^2C_n^2(xL)\,\ell_o^{-7/3}(xL) \quad . \tag{38}$$

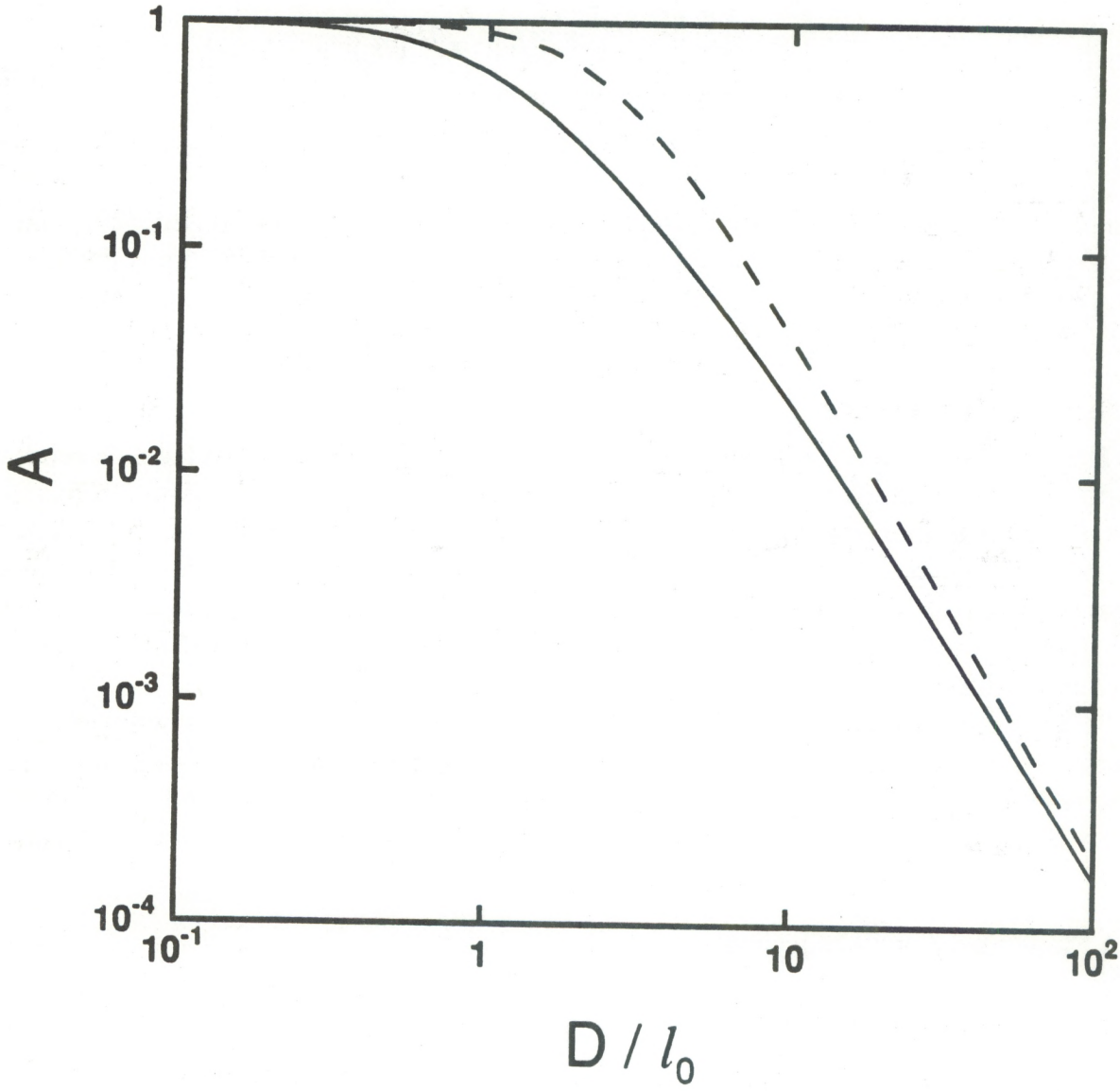

Figure 5. Aperture-averaging factor A vs. ratio of aperture diameter D to inner scale ℓ_0 for spherical-wave propagation through weak turbulence with large inner scale. The solid line is the exact formula, and the dashed line is the recommended approximation.

The aperture-averaging factor is given by

$$A = [1 + 0.109\ C\ D^{7/3}]^{-1}\ , \tag{39}$$

where

$$C = \frac{\int_0^1 dx\ x^2(1-x)^2\ C_n^2(xL)\ \ell_0^{-7/3}(xL)}{\int_0^1 dx\ x^2(1-x)^2\ C_n^2(xL)}\ . \tag{40}$$

For spherical-wave propagation, the small-inner-scale approximation [Eq. (29)] and the large-inner-scale approximation [Eq. (37)] are equal for ℓ_0 equal 1.5 times the Fresnel zone. Therefore, we recommend using the small-inner-scale approximation for $\ell_0 < 1.50(L/k)^{1/2}$ and the large-inner-scale approximation for $\ell_0 > 1.50(L/k)^{1/2}$.

2.2 Strong Turbulence

The strong-turbulence regime is defined as the case where the transverse coherence length of the field in the receiver plane is much smaller than the Fresnel zone. In this case, the covariance contains two scales. A small-scale peak with a width of about the coherence length accounts for $(\sigma_I^2 + 1)/2$ of the covariance, where σ_I^2 is the total irradiance variance. The rest is contained in a long tail with a width of about the scattering disk size. The shape of the covariance is strongly affected by multiple scattering, and analysis is much more difficult than for the weak-scattering case.

Perhaps the asymptotic theory is the best available. For a pure power-law spectrum, this theory has been developed for plane-wave[20] and spherical-wave[21] propagation, and these results are reviewed in Ref. 22. Inner-scale effects have been included in more recent work.[23,24] The covariance function typically used is the sum of three terms of a series expansion.

2.2.1 Plane wave, small inner scale

The asymptotic formula for the covariance function in this case is[22]

$$C_I(\varrho) = \exp\left[\left(\frac{\varrho}{\varrho_0}\right)^{5/3}\right] + \frac{1}{2}\ N_3\left(\frac{k\varrho_0^2}{L}\right)^{1/3}[b_1(\varrho) + b_2(\varrho)]\ , \tag{41}$$

where ϱ_0 is the transverse coherence length calculated using geometrical optics for plane-wave propagation:

$$\varrho_0 = (1.46\ k^2\ L\ C_n^2)^{-3/5}\ . \tag{42}$$

N_3 is a constant given by

$$N_3 = \frac{9(2)^{5/3}}{5\pi}\ \sin\left(\frac{5\pi}{6}\right)\Gamma^2\left(\frac{11}{6}\right)\Gamma\left(\frac{7}{5}\right){}_2F_1\left(\frac{7}{5}, \frac{2}{3}; \frac{5}{3}; \frac{5}{8}\right) = 1.22\ , \tag{43}$$

where Γ represents the gamma function and ${}_2F_1$ the confluent hypergeometric function.[25] The two functions b_1 and b_2 are functions of ϱ that go to unity as ϱ goes to zero, and to zero as ϱ goes to infinity. b_1 is given by

$$b_1(\varrho) = \frac{7}{3}\int_0^1 dx\, x^{4/3}\, J_0(k\ \varrho\ \varrho_0\, x/L)\ . \tag{44}$$

The other function, b_2, is much more complex. We do know that it is a correction to the first term that depends only on the ratio ϱ/ϱ_0 and that it has a characteristic scale size of about ϱ_0. We will assume that b_2 can be reasonably approximated by

$$b_2 = \exp\left[-\left(\frac{\varrho}{\varrho_0}\right)^{5/3}\right]. \tag{45}$$

The variance of irradiance is therefore given by

$$\sigma_I^2 = C_I(0) = 1 + 1.22\left(\frac{k\varrho_0^2}{L}\right)^{1/3}\ . \tag{46}$$

The aperture-averaging factor is the sum of two terms

$$A_1 = \frac{16}{\pi}\frac{\sigma_I^2 + 1}{2\sigma_I^2}\int_0^1 dy\, y\, [\cos^{-1} y - y\,(1-y^2)^{1/2}]\, \exp\left[-\left(\frac{Dy}{\varrho_0}\right)^{5/3}\right], \tag{47}$$

and

$$A_2 = \frac{56L^2}{3k^2D^2\varrho_0^2}\frac{\sigma_I^2 - 1}{2\sigma_I^2}\int_0^1 dx\, x^{-2/3}\, J_1^2\left(\frac{kD\varrho_0 x}{2L}\right). \tag{48}$$

The aperture-averaging factor $A = A_1 + A_2$ is plotted as a function of $D/2\varrho_0$ for several values of σ_I^2 in Fig. 6. In all cases, the effects of the two scale sizes are evident. Since variance decreases with increasing turbulence strength in this regime, the weakest turbulence case presented is the one with the largest variance, $\sigma_I^2 = 1.75$. This value corresponds to a ratio of Fresnel zone size to ϱ_0 of 2.07 from Eq. (46). The scattering disk $L/k\varrho_0$ is therefore $4.3\varrho_0$ for this case. The figure clearly shows the averaging of the ϱ_0 scale, a shoulder, and then a second rolloff about a factor of 4.3 higher. Note also that there is less aperture averaging (e.g., A is higher) than the weak-turbulence theory would predict for this case where $(L/k)^{1/2} = 2.07\varrho_0$. As an example, we see that $D/2\varrho_0 = 10$ implies that $A = 0.109$. The corresponding low-turbulence theory point would be $(kD^2/4L)^{1/2} = 4.83$. Weak-turbulence theory would predict $A = 0.0231$, which is much lower than the actual value.

For $\sigma_I^2 = 1.5$, the Fresnel zone size is about $3.81\ \varrho_0$ and the weak-turbulence theory is even worse. The two scales, ϱ_0 and scattering disk, differ by a factor of 14.5 in this case. The greater separation is evident in Fig. 6.

Finally, the strongest-turbulence case, with $\sigma_I^2 = 1.25$, has a Fresnel zone size that is $10.8\ \varrho_0$. The two scales are separated by a factor of 116. Also note that as turbulence

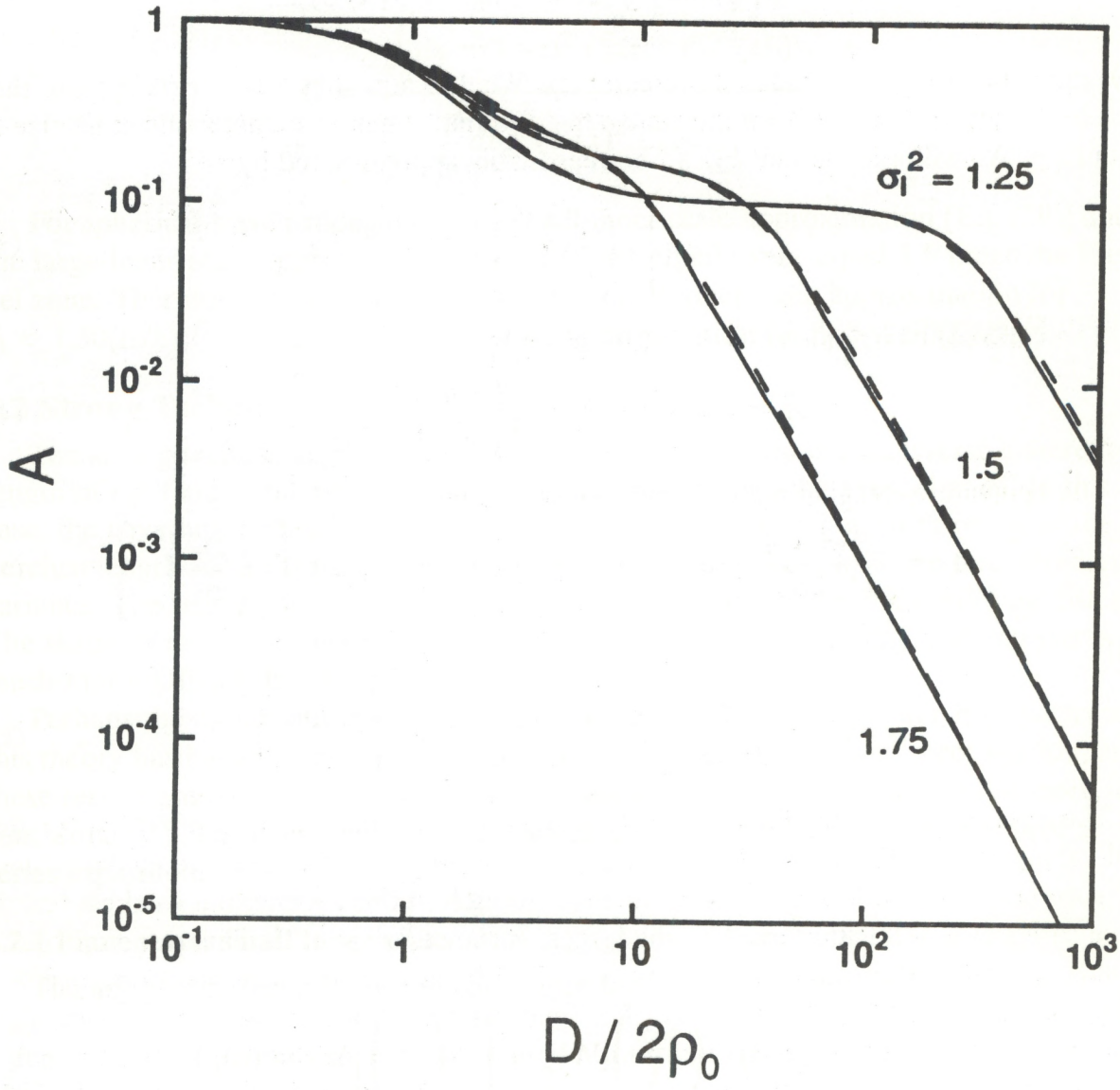

Figure 6. Aperture-averaging factor A vs. ratio of aperture radius $D/2$ to phase coherence length ϱ_0 for plane-wave propagation through strong turbulence with small inner scale and three different values of irradiance variance σ_I^2. The solid lines are the exact results, and the dashed lines represent the recommended approximation.

gets stronger, the plateau between the two scale sizes gets lower. In the asymptotic limit, σ_I^2 goes to unity and only the ϱ_0 scale remains. However, unrealizable turbulence levels are required for this to occur.

For very small D, the exponential in the first term is nearly always unity, and we have

$$A_1 = \frac{\sigma_I^2 + 1}{2\sigma_I^2} \,. \tag{49}$$

For very large D, the integrand will be nearly zero except for very small values of y. Thus, we can evaluate the integral to get

$$A_1 = \frac{\sigma_I^2 + 1}{2\sigma_I^2}\left[1.10\left(\frac{2\varrho_0}{D}\right)^2\right] . \tag{50}$$

As before, we recommend the approximation

$$A_1 = \frac{\sigma_I^2 + 1}{2\sigma_I^2}\left[1 + 0.908\left(\frac{D}{2\varrho_0}\right)^2\right]^{-1} . \tag{51}$$

Note that this term does go as the inverse square of aperture diameter. This is a direct result of the corresponding correlation function being always positive.

For small D, we use the approximation $J_1(a) \approx \frac{1}{2}a$ and get

$$A_2 = \frac{\sigma_I^2 + 1}{2\sigma_I^2} \,. \tag{52}$$

For large D, $J_1^2\,(k\varrho_0\, Dx/2L)$ is nearly zero by the time $x = 1$. Therefore, we can extend the upper limit of integration from 1 to infinity without introducing appreciable error. This integral can be evaluated with the result

$$A_2 = \frac{\sigma_I^2 - 1}{2\sigma_I^2}\left[6.16\left(\frac{2L}{k\varrho_0 D}\right)^{7/3}\right] , \tag{53}$$

and we have the approximation

$$A_2 = \frac{\sigma_I^2 - 1}{2\sigma_I^2}\left[1 + 0.162\left(\frac{k\varrho_0 D}{2L}\right)^{7/3}\right]^{-1} . \tag{54}$$

Summing A_1 and A_2 yields

$$A = \frac{\sigma_I^2 + 1}{2\sigma_I^2}\left[1 + 0.908\left(\frac{D}{2\varrho_0}\right)^2\right]^{-1} + \frac{\sigma_I^2 - 1}{2\sigma_I^2}\left[1 + 0.162\left(\frac{k\varrho_0 D}{2L}\right)^{7/3}\right]^{-1} , \tag{55}$$

which is plotted in Fig. 6 along with the exact theory. We note very good agreement between the approximation and the exact values over the entire range of aperture diameters considered.

Evaluation of the correlation function for the case where C_n^2 varies along the path is extremely difficult in strong turbulence, and the aperture-averaging factor could not be obtained. We note that the phase coherence length in this case is

$$\varrho_0 = \left[1.46\, k^2 \int_0^L dz\; C_n^2(z)\right]^{-3/5} . \tag{56}$$

Using this in Eq. (55) may produce reasonable approximations, although this is merely conjecture.

2.2.2 Plane wave, large inner scale

If the inner scale is much larger than the coherence length, but much smaller than the scattering disk, the asymptotic theory yields[23]

$$C_I(\varrho) = \exp\left[-\left(\frac{\varrho}{\varrho_0}\right)^2\right] + \frac{1}{2} N_3 \left(\frac{k\varrho_0 \ell_0}{L}\right)^{1/3} [b_1(\varrho) + b_2(\varrho)] , \tag{57}$$

where

$$\varrho_0 = (1.20\, k^2\, C_n^2\, L\, \ell_0^{-1/3})^{-1/2} , \tag{58}$$

and $N_3 = 1.21$. The function $b_1(\varrho)$ is given by

$$b_1(\varrho) = 0.897 \left(\frac{L}{k\varrho_0}\right)^{7/3} \int_0^1 d\tau\; \tau^2 \int_0^\infty dK\; K^{4/3} \exp\left[-\frac{L^2}{k^2\varrho_0^2} K^2\tau^2 \left(1 - \frac{2}{3}\tau\right)\right] J_0(K\varrho) . \tag{59}$$

The other function b_1 is again an extremely complex function. As before, we will assume

$$b_2(\varrho) = \exp\left[-\left(\frac{\varrho}{\varrho_0}\right)^2\right] . \tag{60}$$

The variance of irradiance is given by

$$\sigma_I^2 = 1 + 1.21 \left(\frac{k\varrho_0 \ell_0}{L}\right)^{1/3} . \tag{61}$$

The aperture-averaging factor is again the sum of two terms

$$A_1 = \frac{16}{\pi} \frac{\sigma_I^2 + 1}{2\sigma_I^2} \int_0^1 dy\; y[\cos^{-1} y - y(1 - y^2)^{1/2}] \exp[-(Dy/\varrho_0)^2] , \tag{62}$$

and

$$A_2 = 3.59 \left(\frac{2L}{k\varrho_0 D}\right)^{7/3} \frac{\sigma_I^2 - 1}{2\sigma_I^2} \int_0^1 d\tau\, \tau^2 \int_0^\infty du\, u^{-2/3} J_1^2(u) \times \exp\left[-\left(\frac{2L}{k\varrho_0 D}\right)^2 u^2 \tau^2 \left(1 - \frac{2}{3}\tau\right)\right]. \tag{63}$$

The total aperture-averaging factor $A = A_1 + A_2$ is plotted as a solid line in Fig. 7 for several values of σ_I^2 and for the special case of $\ell_0 = 10\varrho_0$.

For very small D, the exponential in Eq. (62) is nearly always unity and we have

$$A_1 = \frac{\sigma_I^2 + 1}{2\sigma_I^2}. \tag{64}$$

For very large D, $\cos^{-1}y - y(1-y^2)^{1/2}$ can be approximated by its value at $y = 0$, which is $\pi/2$. The integral can then be evaluated to yield

$$A_1 = \frac{\sigma_I^2 + 1}{2\sigma_I^2}\left(\frac{2\varrho_0}{D}\right)^2, \tag{65}$$

and we have the approximation

$$A_1 = \frac{\sigma_I^2 + 1}{2\sigma_I^2}\left[1 + \left(\frac{D}{2\varrho_0}\right)^2\right]^{-1}. \tag{66}$$

For small D, we can use the approximation $J_1(a) \approx \frac{1}{2}a$ in Eq. (63), and we get

$$A_2 = \frac{\sigma_I^2 - 1}{2\sigma_I^2}. \tag{67}$$

For large D, the exponential in Eq. (63) can be approximated by one, which leads to

$$A_2 = \frac{\sigma_I^2 - 1}{2\sigma_I^2}\left[0.790\left(\frac{2L}{k\varrho_0 D}\right)^{7/3}\right], \tag{68}$$

so that we have the approximation

$$A_2 = \frac{\sigma_I^2 - 1}{2\sigma_I^2}\left[1 + 1.27\left(\frac{k\varrho_0 D}{2L}\right)^{7/3}\right]^{-1}. \tag{69}$$

Therefore,

$$A = \frac{\sigma_I^2 + 1}{2\sigma_I^2}\left[1 + \left(\frac{D}{2\varrho_0}\right)^2\right]^{-1} + \frac{\sigma_I^2 - 1}{2\sigma_I^2}\left[1 + 1.27\left(\frac{k\varrho_0 D}{2L}\right)^{7/3}\right]^{-1}. \tag{70}$$

This is plotted as a dashed line in Fig. 7. As before, agreement is very good.

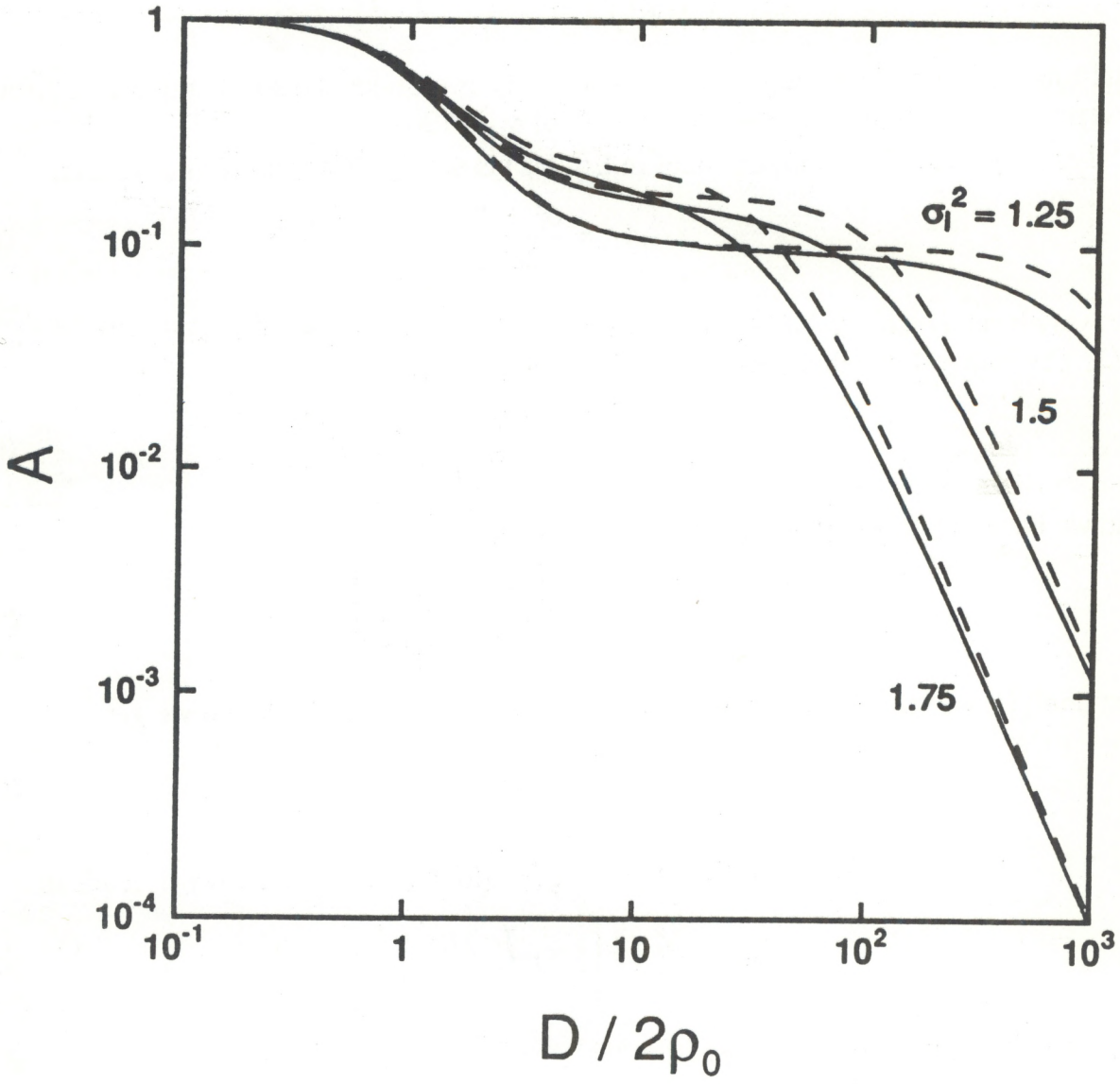

Figure 7. Aperture-averaging factor A vs. ratio of aperture radius $D/2$ to phase coherence length ϱ_0 for plane-wave propagation through strong turbulence with $\ell_0 = 10\,\varrho_0$ and three different values of irradiance variance σ_I^2. The solid lines are the exact results, and the dashed lines represent the recommended approximation.

If the inner scale is yet larger (much larger than the scattering disk), the variance of irradiance can be approximated by

$$\sigma_I^2 = 1 + 10.6\left(\frac{L}{k\varrho_0\ell_0}\right)^2 . \tag{71}$$

A_1 is still given by Eq. (62). However, A_2 becomes

$$A_2 = \frac{\sigma_I^2 - 1}{2\sigma_I^2}(1.20)\left(\frac{2L}{k\varrho_0 D}\right)^{7/3}\int_0^\infty du\, u^{-2/3} J_1^2(u) \exp\left[-0.0285\left(\frac{2\ell_0}{D}\right)^2 u^2\right] \tag{72}$$

in this limit. It is clear that the limits of this equation for small and large D values are the same as Eq. (63) and the approximate aperture-averaging factor is still given by Eq. (70).

If turbulence is not constant along the path, we note that ϱ_0 is given by

$$\varrho_0 = \left[1.20\, k^2 \int_0^L dz\, C_n^2(z)\ell_0^{-1/3}(z)\right]^{-1/2} , \tag{73}$$

and this value can be used in the previous equations. How well this represents the actual values remains a subject for further study.

2.2.3 Spherical wave, small inner scale

The covariance function for this case can be expressed in the same form as the plane-wave, small-inner-scale case, given in Eq. (41).[22] However, we have here

$$\varrho_0 = (0.545\, k^2\, L\, C_n^2)^{-3/5} , \tag{74}$$

and

$$N_3 = \frac{3(2)^{8/3}}{5\pi}\left(\frac{8}{3}\right)^{7/5}\sin\left(\frac{5\pi}{6}\right)\Gamma^2\left(\frac{11}{6}\right)\Gamma\left(\frac{7}{5}\right)\Gamma^2\left(\frac{2}{3}\right)/\Gamma\left(\frac{4}{3}\right) = 3.86 . \tag{75}$$

The function b_1 is given by [21]

$$b_1(\varrho) = 0.915\int_0^1 dx\, x^{-1/3}(1-x)^2\int_0^\infty d\tau\, \tau^{4/3} J_0\left(\frac{k\varrho\varrho_0\tau}{L}\right)\exp[-\tau^{5/3}(1-x)^{5/3}] . \tag{76}$$

As before, the function b_2 is extremely difficult to evaluate, and we will assume that it has the form

$$b_2(\varrho) = \exp\left[-\left(\frac{\varrho}{\varrho_0}\right)^{5/3}\right] . \tag{77}$$

The variance of irradiance is given by

$$\sigma_I^2 = 1 + 3.86\left(\frac{k\varrho_0^2}{L}\right)^{1/3} . \tag{78}$$

The aperture-averaging factor is the sum of

$$A_1 = \frac{16}{\pi}\frac{\sigma_I^2+1}{2\sigma_I^2}\int_0^1 dy\; y[\cos^{-1}y - y(1-y^2)^{1/2}]\exp\left[-\left(-\frac{Dy}{\varrho_0}\right)^{5/3}\right], \tag{79}$$

and

$$A_2 = 3.66\left(\frac{2L}{kD\varrho_0}\right)^{7/3}\frac{\sigma_I^2-1}{2\sigma_I^2}\int_0^\infty du\; u^{-2/3}J_1^2(u)\int_0^1 dx\; x^2(1-x)^{-1/3} \times \exp\left[-\left(\frac{2L}{kD\varrho_0}\right)^{5/3}u^{5/3}\,x^{5/3}\right]. \tag{80}$$

The aperture-averaging factor $A = A_1 + A_2$ is plotted as a solid line in Fig. 8 for several values of the irradiance variance σ_I^2. Qualitatively, these curves are very similar to the plane-wave case. The two scales do tend to be more widely separated in spherical-wave propagation than in plane-wave propagation.

The limits can be found for large and small apertures in the same manner as before. This leads to the recommended approximation

$$A = \frac{\sigma_I^2+1}{2\sigma_I^2}\left[1 + 0.908\left(\frac{D}{2\varrho_0}\right)^2\right]^{-1} + \frac{\sigma_I^2-1}{2\sigma_I^2}\left[1 + 0.613\left(\frac{kD\varrho_0}{2L}\right)^{7/3}\right]^{-1}. \tag{81}$$

This is plotted as a dashed line in Fig. 8. Once again, the approximation is good. However, as in the weak-turbulence cases, the approximation for spherical-wave propagation is not as good as for plane-wave propagation for apertures near the Fresnel zone.

2.2.4 Spherical wave, large inner scale

We first treat the case where the inner scale is much larger than the coherence length but much smaller than the scattering disk. For this case, the asymptotic theory expression for the covariance can be written in the same form as the plane-wave equivalent of Eq. (57). However, here we have

$$\varrho_0 = (0.545\; k^2\; C_n^2\; L\; \ell_0^{-1/3})^{-1/2}, \tag{82}$$

and $N_3 = 1.13$. The function b is given by

$$b_1(\varrho) = 1.05\left(\frac{L}{k\varrho_0}\right)^{7/3}\int_0^1 dx\; x^2(1-x)^2\int_0^\infty dK\; K^{4/3}\exp\left[-\frac{L^2}{k^2\varrho_0^2}K^2x^2(1-x)^2\right]J_0(Kx\varrho). \tag{83}$$

We will again assume

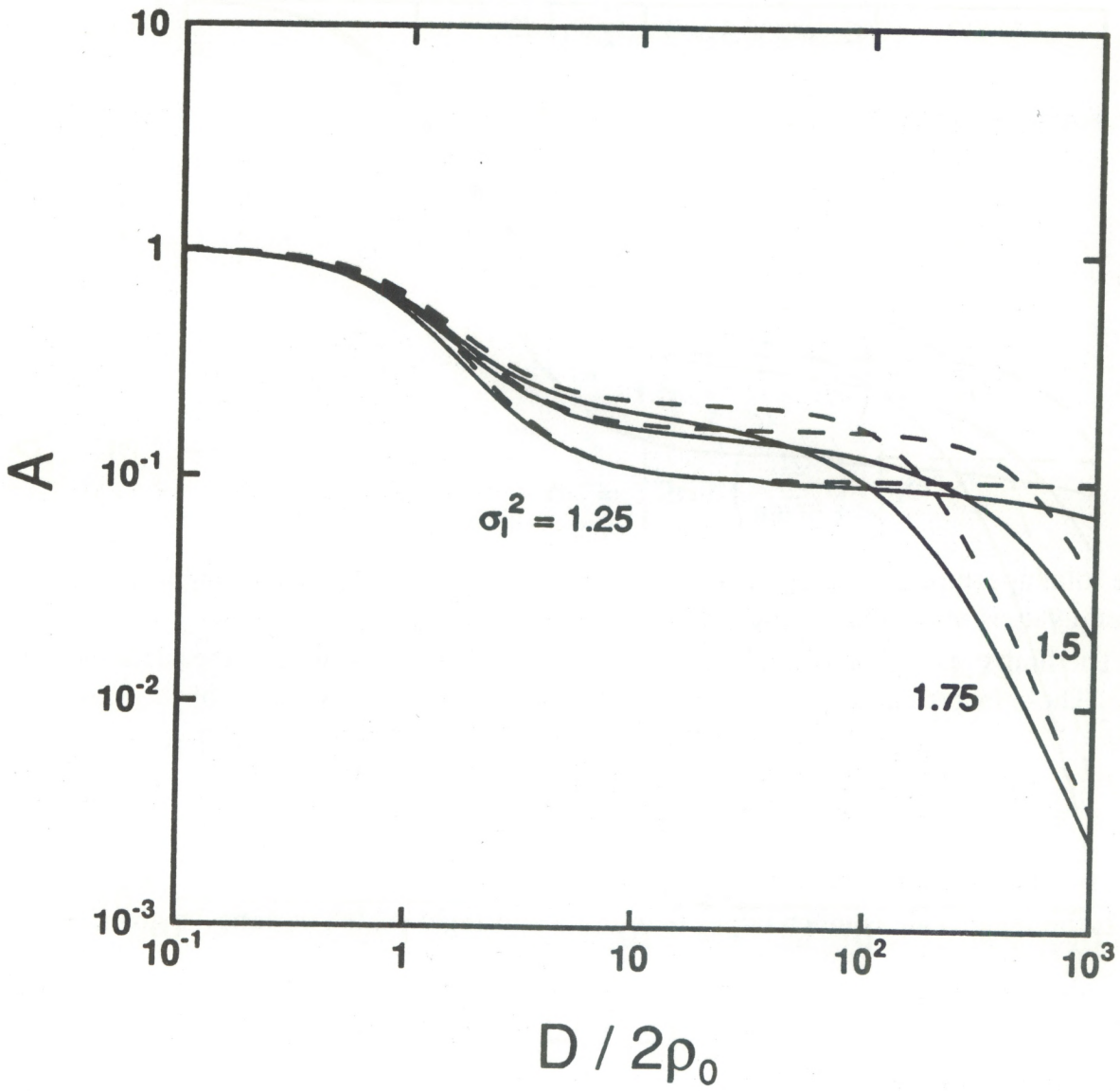

Figure 8. Aperture-averaging factor A vs. ratio of aperture radius $D/2$ to phase coherence length ϱ_0 for spherical-wave propagation through strong turbulence and three different values of irradiance variance σ_I^2. The solid lines are the exact results, and the dashed lines represent the recommended approximation.

$$b_2(\varrho) = \exp\left[-\left(\frac{\varrho}{\varrho_0}\right)^2\right]. \tag{84}$$

The variance of irradiance in this approximation is given by

$$\sigma_I^2 = 1 + 2.27\left(\frac{k\varrho_0\ell_0}{L}\right)^{1/3}. \tag{85}$$

The aperture-averaging factor is the sum of the two terms

$$A_1 = \frac{16}{\pi}\frac{\sigma_I^2 + 1}{2\sigma_I^2}\int_0^1 dy\; y\; [\cos^{-1} y\; y\; (1-y^2)^{1/2}]\; \exp\left[-\left(-\frac{Dy}{\varrho_0}\right)^2\right], \tag{86}$$

and

$$A_2 = 4.20\left(\frac{2L}{kD\varrho_0}\right)^{7/3}\frac{\sigma_I^2 - 1}{2\sigma_I^2}\int_0^1 dx\; x^2(1-x)^{-1/3}\int_0^\infty du\; u^{-2/3}J_1^2(u) \times \exp\left[-\left(\frac{2L}{kD\varrho_0}\right)^2 x^2\, u^2\right]. \tag{87}$$

The total aperture-averaging factor $A = A_1 + A_2$ is plotted as a solid line in Fig. 9 for several values of σ_I^2 and for the special case of $\ell_0 = 10\varrho_0$.

The limits of large and small aperture diameter can be taken as in the plane-wave case. These lead to an approximation for the aperture-averaging factor of

$$A = \frac{\sigma_I^2 + 1}{2\sigma_I^2}\left[1 + \left(\frac{D}{2\varrho_0}\right)^2\right]^{-1} + \frac{\sigma_I^2 - 1}{2\sigma_I^2}\left[1 + 0.534\left(\frac{kD\varrho_0}{2L}\right)^{7/3}\right]^{-1}. \tag{88}$$

This function is plotted as a dashed line in Fig. 9.

If the inner scale is much larger than the scattering disk, the variance is given by

$$\sigma_I^2 = 1 + 2.34\left(\frac{L}{k\varrho_0\ell_0}\right)^2. \tag{89}$$

A_1 is still given by Eq. (87). However, A_2 becomes

$$A_2 = 4.20\left(\frac{2L}{kD\varrho_0}\right)^{7/3}\frac{\sigma_I^2 - 1}{2\sigma_I^2}\int_0^1 dx\; x^2(1-x)^{-1/3}\int_0^\infty du\; u^{-2/3}J_1^2(u) \times \exp\left[-0.0285\left(\frac{2\ell_0}{D}\right)^2 u^2/x^2\right]. \tag{90}$$

This has the same limits as Eq. (87) and the approximate formula is still given by Eq. (88).

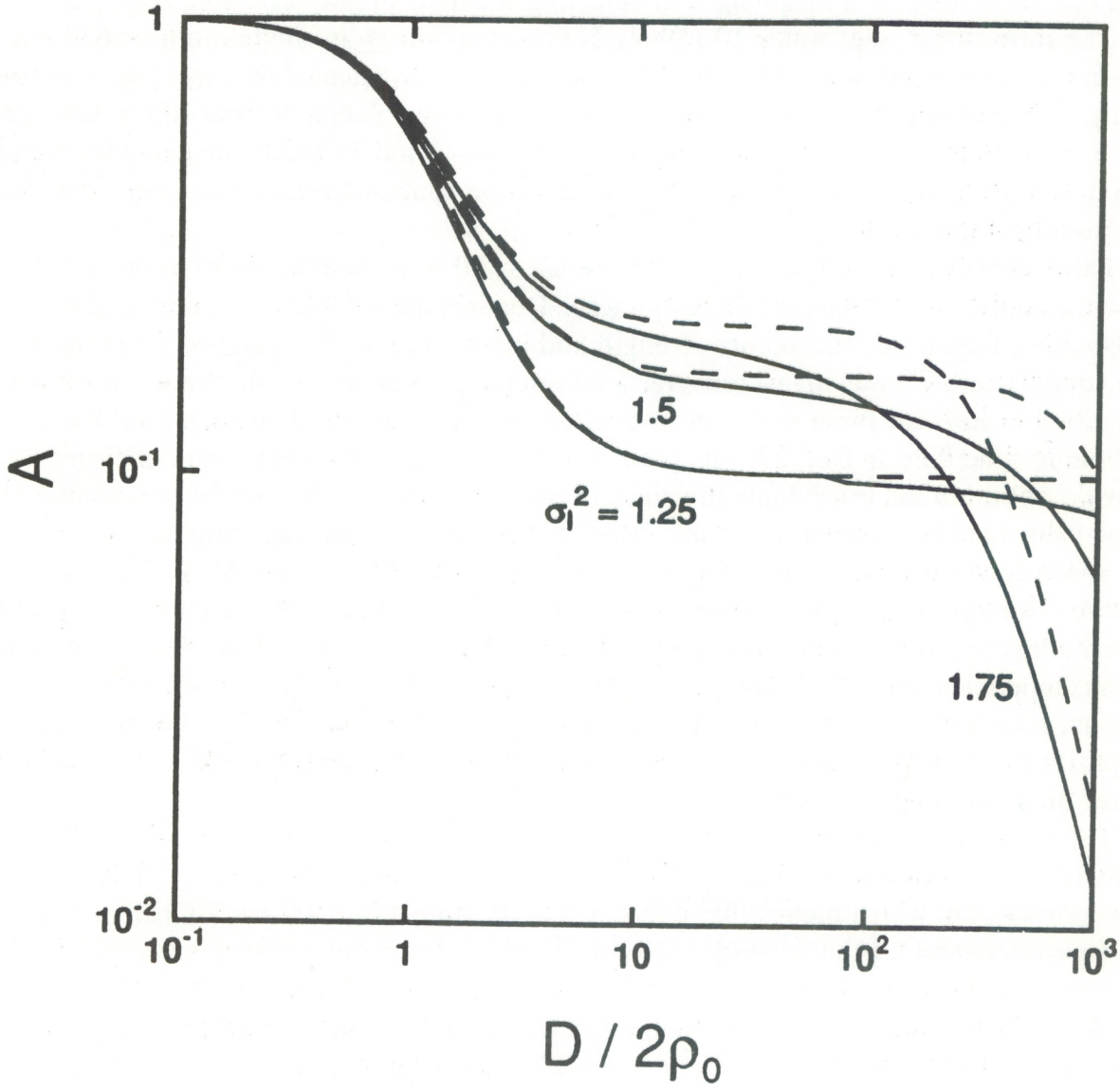

Figure 9. Aperture-averaging factor A vs. ratio of aperture radius $D/2$ to phase coherence length ϱ_0 for spherical-wave propagation through strong turbulence with $\ell_0 = 10\,\varrho_0$ and three different values of irradiance variance σ_I^2. The solid lines are the exact results, and the dashed lines represent the recommended approximation.

3. EXPERIMENT

A series of experiments was performed to verify some of these relationships. Not all parameter regimes were possible, but an attempt was made to investigate as many as possible. The experiments involved propagating a laser transmitter over some distance through the turbulent atmosphere and detecting the light with a variety of aperture sizes.

The transmitter laser was a 10-mW HeNe laser operating in single mode at 633 nm. When the path length was 1 km, the 1.2-mrad beam divergence of the laser was used directly. When shorter paths were used, a negative lens was placed in front of the laser so that the beam at the receiver had a diameter of about 1 m. An electromechanical shutter was placed in front of the lens. This shutter could be controlled from the receiver end of the path by a radio link.

Paths of 100, 250, 500, and 1000 m were used. All were at a height of about 1.5 m over flat, uniform grassland at the Commerce Department's Table Mountain facility north of Boulder, Colorado. Turbulence strength and inner scale were measured using optical instrumentation. C_n^2 was measured over a 500-m path, using an incoherent scintillometer described in Ref. 26. Inner scale was measured over a 150-m path, using a scintillation technique described in Ref. 27. The path lengths for both instruments were chosen to provide optimum measurements. Because of the uniformity of the terrain, we assume that these values are representative of the values along the actual propagation paths.

The receiver is an array of six apertures with diameters of 1, 2.25, 5, 10, 25, and 50 mm. The light passing through each aperture is detected by a photodiode; except for the smallest aperture, a lens is used to collect the light. Each photodiode is connected to a transimpedance amplifier. The gain of each amplifier is inversely proportional to aperture area so that the output signal levels are roughly equivalent. The bandwidth of each amplifier is set at about 5 kHz. The outputs are further amplified and fed to the A/D converter on a personal computer.

The computer software first samples the six detector channels sequentially, with a delay of 36 μs between channels. This sampling is repeated 30,000 times at 500 repetitions per second, which means that each channel is sampled at 500 Hz for 1 min. Then, the computer samples the current values of C_n^2 and ℓ_0 from those instruments. Next, a radio signal is sent from the computer to the transmitter to close the shutter, and the detector channels are sampled for 0.6 s (300 samples/channel) to obtain background levels. The collected data are stored on the computer's disk, a signal is sent to open the shutter, and the entire cycle is repeated. A typical data run consisted of 25 of these cycles and took about 30 min. Data were stored on magnetic tape for later processing.

The data were processed one cycle at a time. First the mean background level was found for each aperture. Then this level was subtracted from each of the data points, and the mean and variance of the result were calculated. The variance was then normalized by the square of the mean. Finally, the aperture-averaging factor was estimated by assuming that the 1-mm aperture provided a fair representation of the unaveraged variance and by dividing the normalized variance from each of the other apertures by this value.

3.1 Weak Turbulence Results

The first data run we consider was obtained over a propagation path of 100 m. Turbulence strength was moderate, with $C_n^2 = 5.19 \pm 1.54 \times 10^{-14} \mathrm{m}^{-2/3}$. The normalized variance of irradiance measured using the 1-mm aperture was $7.21 \pm 1.47 \times 10^{-3}$, and we are clearly in the weak turbulence regime. Reported uncertainties and error bars represent the standard deviation of the values from the 25 cycles that make up each data run. They should be interpreted as variations in atmospheric conditions rather than as measurement errors. The 100-m path length implies a Fresnel zone size of $(L/k)^{1/2} =$ 3.17 mm. The measured inner scale was $\ell_0 = 6.26 \pm 0.38$mm. Since $\ell_0 > 1.5(L/k)^{1/2}$, the large-inner-scale theory is appropriate for these data. The measured aperture-averaging factor A is plotted as a function of D/ℓ_0, including error bars on A and on D/ℓ_0, in Fig. 10. The approximate theory for spherical wave propagation through weak turbulence with large inner scale (37) is plotted as a solid line in the figure. We see very good agreement between the approximate theory and the measured values.

The next data to consider were taken at 250 m with a turbulence level of $1.12 \pm 0.43 \times 10^{-13} \mathrm{m}^{-2/3}$. The variance for the 1-mm aperture was $6.81 \pm 4.47 \times 10^{-2}$, and we are still in the weak turbulence regime. The Fresnel zone size for this case is 5.02 mm. The measured inner scale was 7.54 ± 1.22 mm, and the average value of $\ell_0 \approx 1.5(L/k)^{1/2}$. Fig. 11 presents the data for this case along with the spherical wave, weak turbulence, large-inner-scale theory of Eq. (37). Again we see good agreement between theory and data. Fig. 12 presents the same data, plotted as a function of $(kD^2/4L)^{1/2}$. Note that the Fresnel zone is independent of atmospheric conditions, and only vertical error bars are presented in this figure. The solid line in this case is the approximate theory for spherical wave propagation through weak turbulence with a small inner scale (29). We see that the agreement is almost identical to that of Fig. 11, supporting our conjecture that either theory can be used when $\ell_0 \approx 1.5(L/k)^{1/2}$.

The data for Fig. 13 were taken at 500 m. C_n^2 was $1.46 \pm 1.18 \times 10^{-13}$ $\mathrm{m}^{-2/3}$. The 1-mm aperture variance for this case was 0.644 ± 0.348 and we are still in weak turbulence, although the margin is smaller than in the previous cases. The Fresnel zone size is 7.10 mm. The inner scale, 7.19 ± 0.90 mm, is about the same size and is thus less than $1.5(L/k)^{1/2}$. Therefore, the data are plotted as a function of $(kD^2/4L)^{1/2}$ and the small-inner-scale theory of Eq. (29) is used for comparison. Again we see good agreement between theory and experiment.

These results show that the approximate formulas provide good agreement to measured values for the aperture-averaging factor of a spherical wave in weak turbulence. Generally, the approximate formulas were somewhat higher than the data near the knee of the wave. This is consistent with the theoretical finding that the approximation was above the exact calculation in this area. The notable exception to this generalization was the 250-m data run presented here. We suspect that the assumption of uniformity was violated during this run because of clouds over part of the sky, and the value for ℓ_0 along the path was greater than the measured value. Despite this, agreement between the data and theory was good.

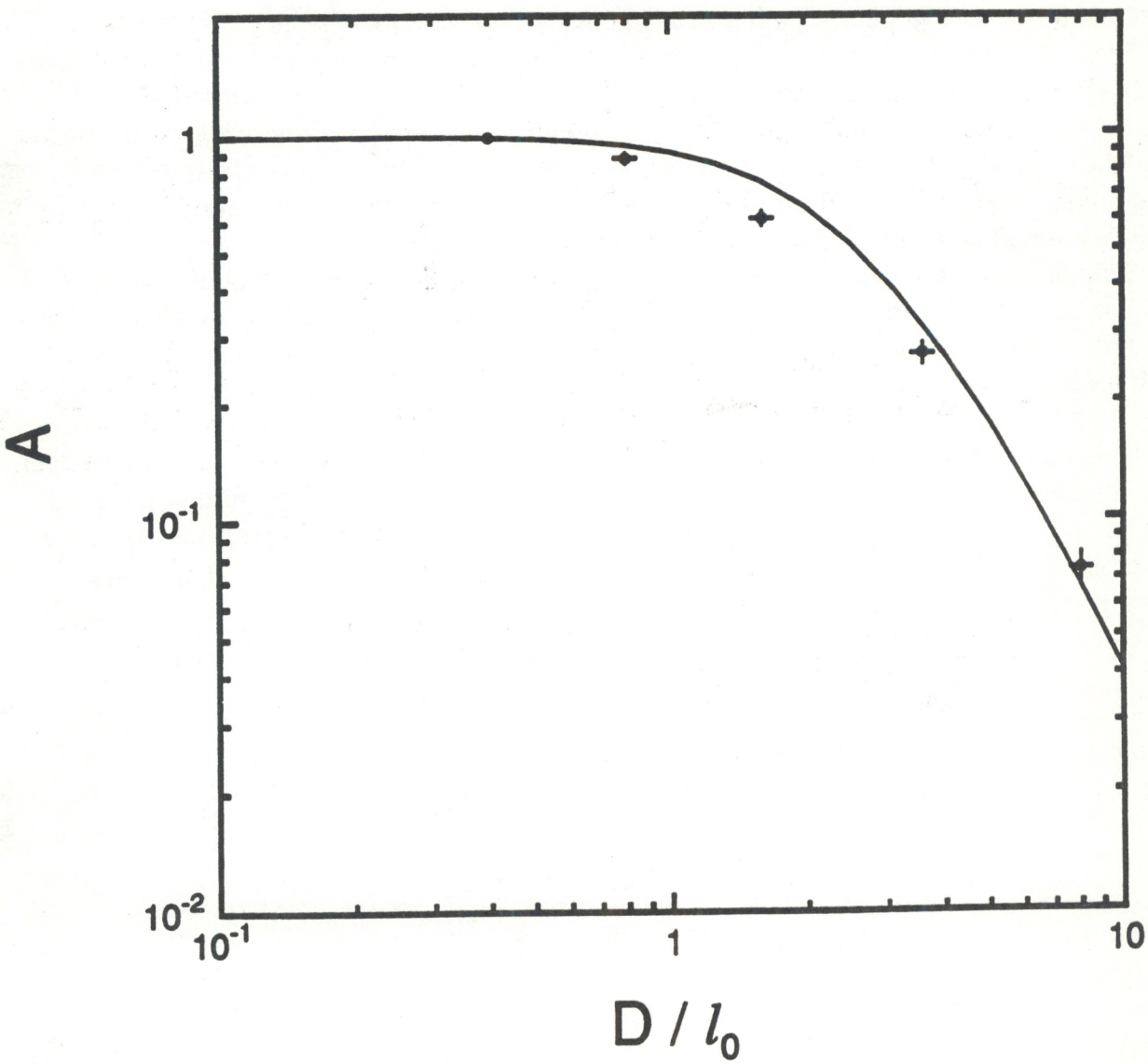

Figure 10. Aperture-averaging factor A vs. ratio of aperture diameter D to inner scale ℓ_0. The points represent data taken at 100 m, and the curve is the approximate formula for a spherical wave, weak turbulence, and large ℓ_0.

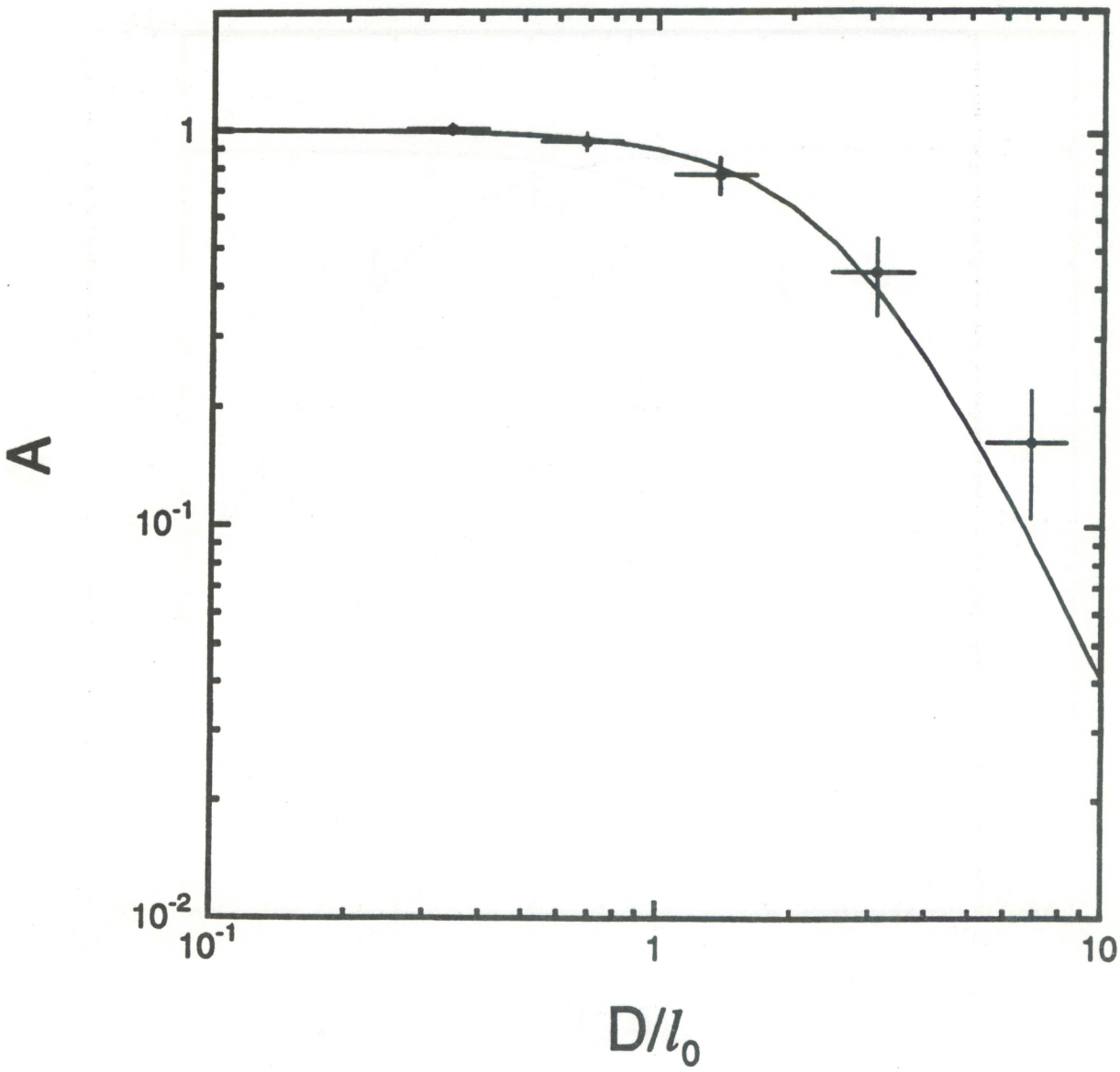

Figure 11. Aperture-averaging factor A vs. ratio of aperture diameter D to inner scale ℓ_0. The points represent data taken at 250 m, and the curve is the approximate formula for a spherical wave, weak turbulence, and large ℓ_0.

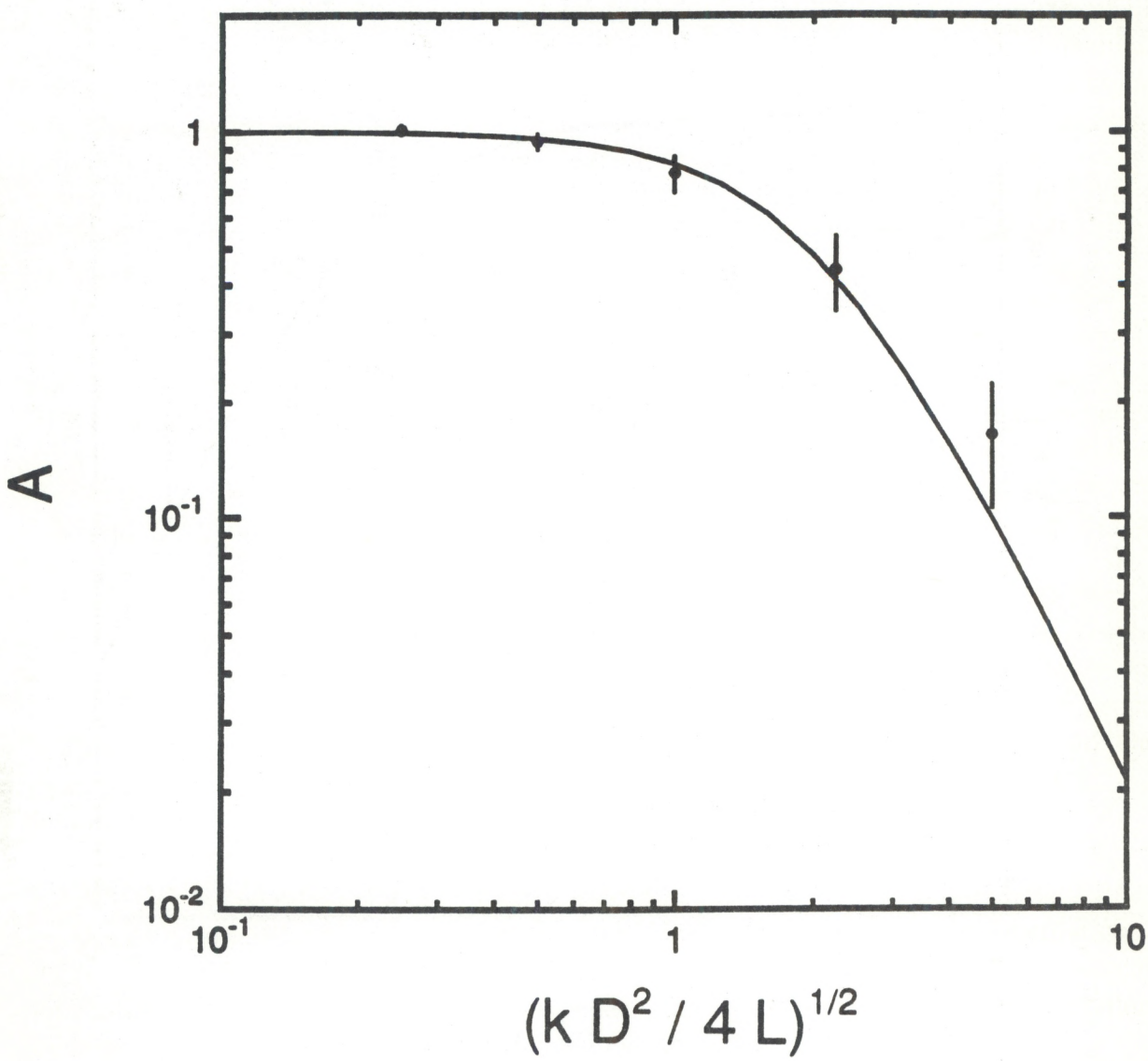

Figure 12. Aperture-averaging factor A vs. ratio of aperture radius $D/2$ to Fresnel zone size $(L/k)^{1/2}$. The points represent data taken at 250 m, and the curve is the approximate formula for a spherical wave, weak turbulence, and small ℓ_0.

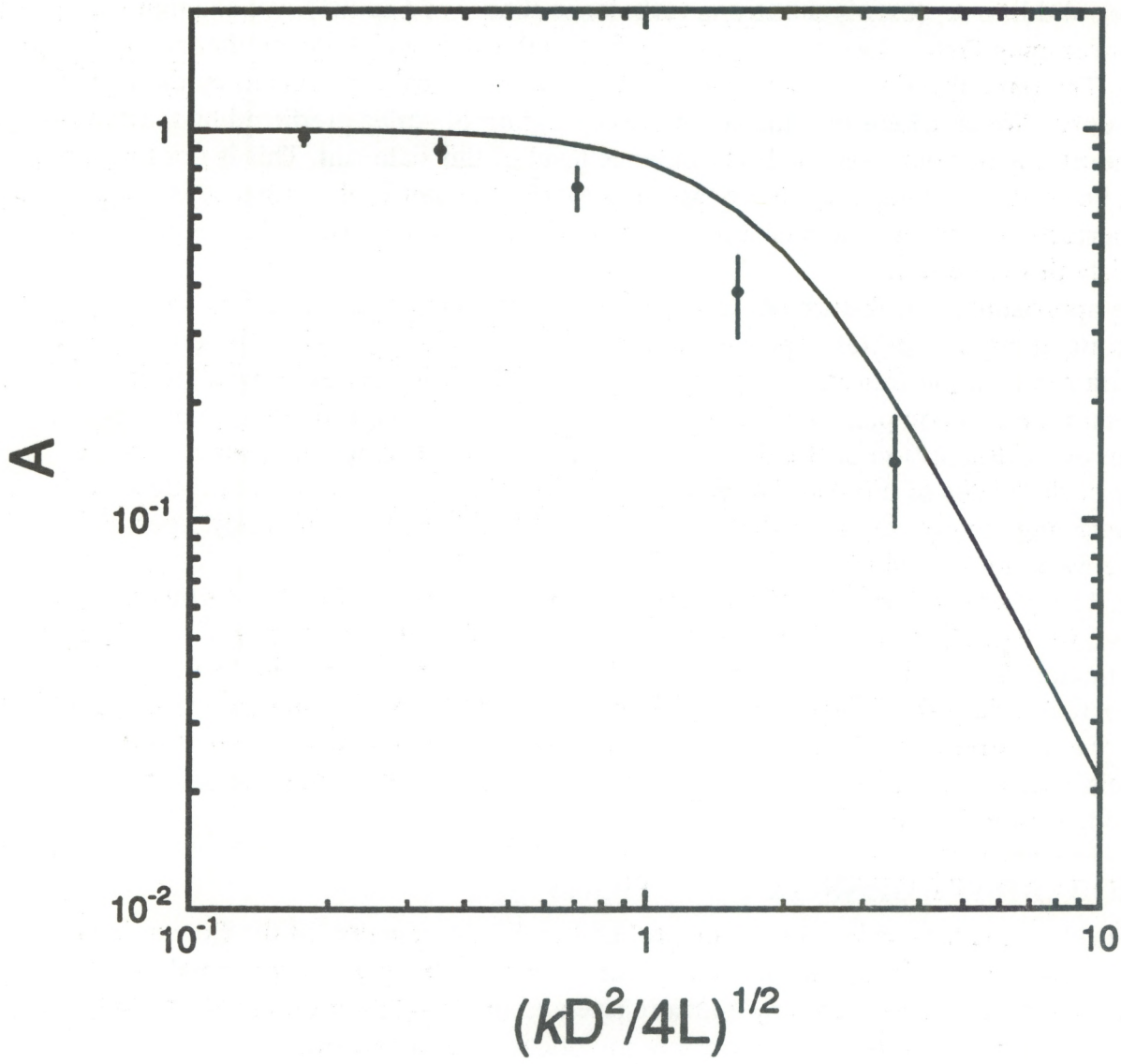

Figure 13. Aperture-averaging factor A vs. ratio of aperture radius $D/2$ to Fresnel zone size $(L/k)^{1/2}$. The points represent data taken at 500 m, and the curve is the approximate formula for a spherical wave, weak turbulence, and small ℓ_0.

3.2 Strong Turbulence Results

Data to investigate the strong path-integrated turbulence regime were collected over a 1000-m path. In the first case, the turbulence strength was $C_n^2 = 4.20 \pm 0.33 \times 10^{-13}$ m$^{-2/3}$. The inner scale $\ell_0 = 5.98 \pm 0.35$ mm, which was larger than the coherence length of $\varrho_0 = 2.84 \pm 0.11$ mm, The Fresnel zone size of $(L/k)^{1/2} = 10.0$ mm was also larger than ϱ_0, and this case is in strong turbulence.

The measured values for A, with error bars, are plotted as a function of $D/2\varrho_0$ in Fig. 14. The solid line represents the strong turbulence theory of Eq. (81). We see that the aperture-averaging factor does not drop off as fast as the strong-turbulence theory would predict. The data also do not show the clear separation of scales predicted by the asymptotic theory. We conclude that the complete separation of scales predicted by the asymptotic theory has not occurred at the turbulence level of this data run. This is not too surprising because the asymptotic theory assumes that the variance of irradiance is 1 plus a small perturbation term. The measured variance of the 1-mm aperture, 3.15 ± 0.24, does not satisfy this condition.

The approximate weak-turbulence theory is given as a dashed line in Fig. 14. The asymptotic theory is a better approximation to the data than the weak-turbulence theory. This data run is in the transition regime between the single-scale size of weak turbulence theory and the two completely separated scale sizes of the asymptotic theory; neither provides an exact description of the data. This is particularly true since our data are in the vicinity of the scales of interest. We expect that very large apertures would produce aperture-averaging factors very near the asymptotic theory values. Unfortunately, apertures of this size were not available.

Fig. 15 presents the results of a similar run under conditions of higher turbulence. In this case, we had $C_n^2 = 1.29 \pm 0.39 \times 10^{-12}$ m$^{-2/3}$, $\ell_0 = 7.57 \pm 0.55$ mm, $\varrho_0 = 1.74 \pm 0.24$ mm, and the variance from the 1-mm aperture was 3.08 ± 0.38. The irradiance variance decreases very slowly with increasing turbulence strength for spherical wave propagation,[18] and extreme conditions are required for the asymptotic theory to be valid. Despite this, reasonable agreement with the measured aperture-averaging factors are obtained, as seen in Fig. 15.

4. PROBABILITY DENSITY FUNCTIONS

The other quantity of interest is the probability density function of the fluctuations of the received power. We expect that these fluctuations will be nearly log normal in weak path-integrated turbulence for any aperture size and in strong path-integrated turbulence for large apertures. These expectations are investigated in this section.

The measured probability histogram of the data taken through a 1-mm aperture at a distance of 100 m is plotted as a function of signal S in Fig. 16. The smooth curve is a log-normal density function with the same variance ($\sigma_S^2 = 7.21 \times 10^{-3}$). The log-normal

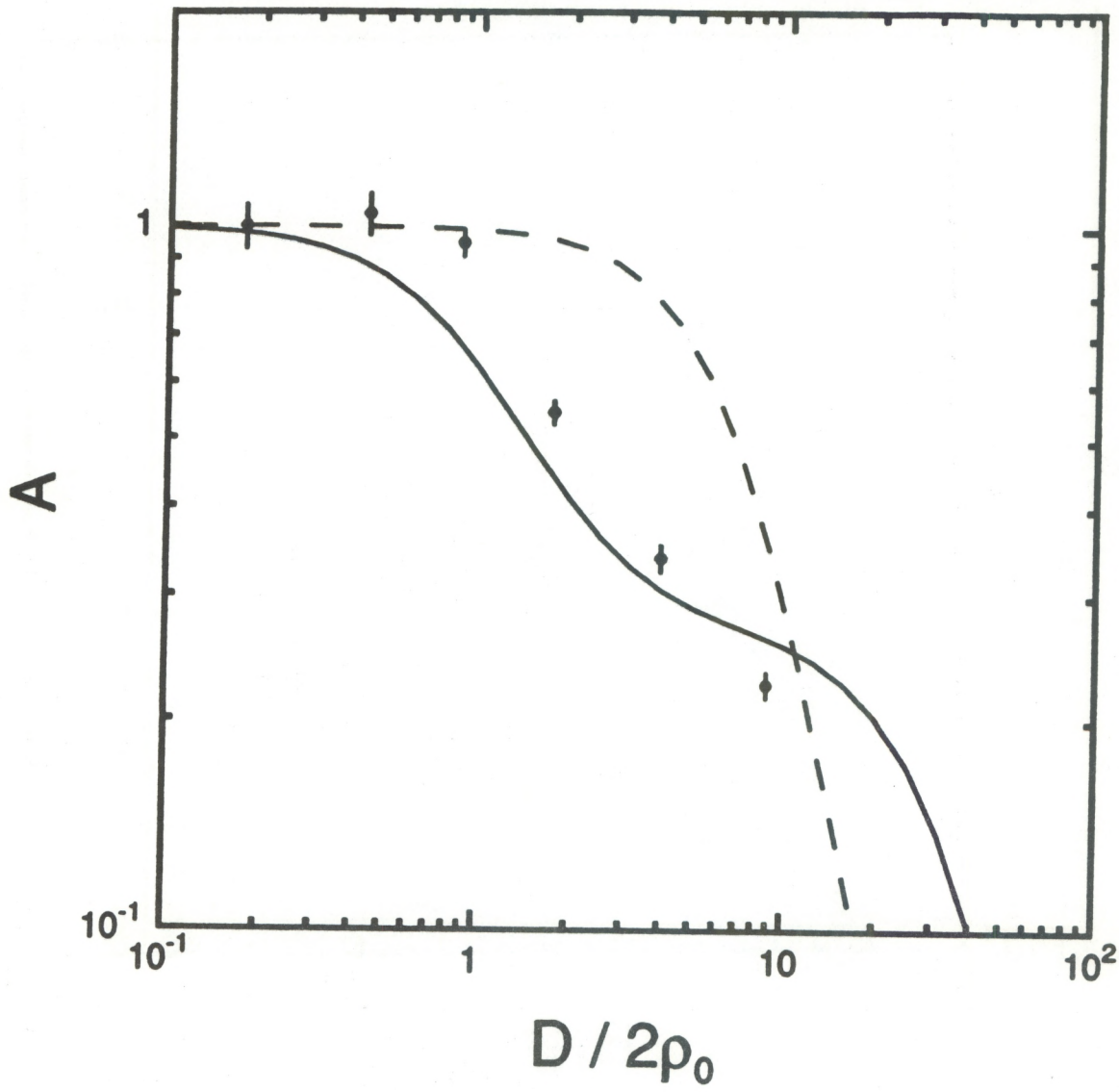

Figure 14. Aperture-averaging factor A vs. ratio of aperture radius $D/2$ to coherence length ϱ_0. The points represent data taken an 1000 m, the solid curve is the strong-turbulence approximation, and the dashed curve is the weak-turbulence approximation.

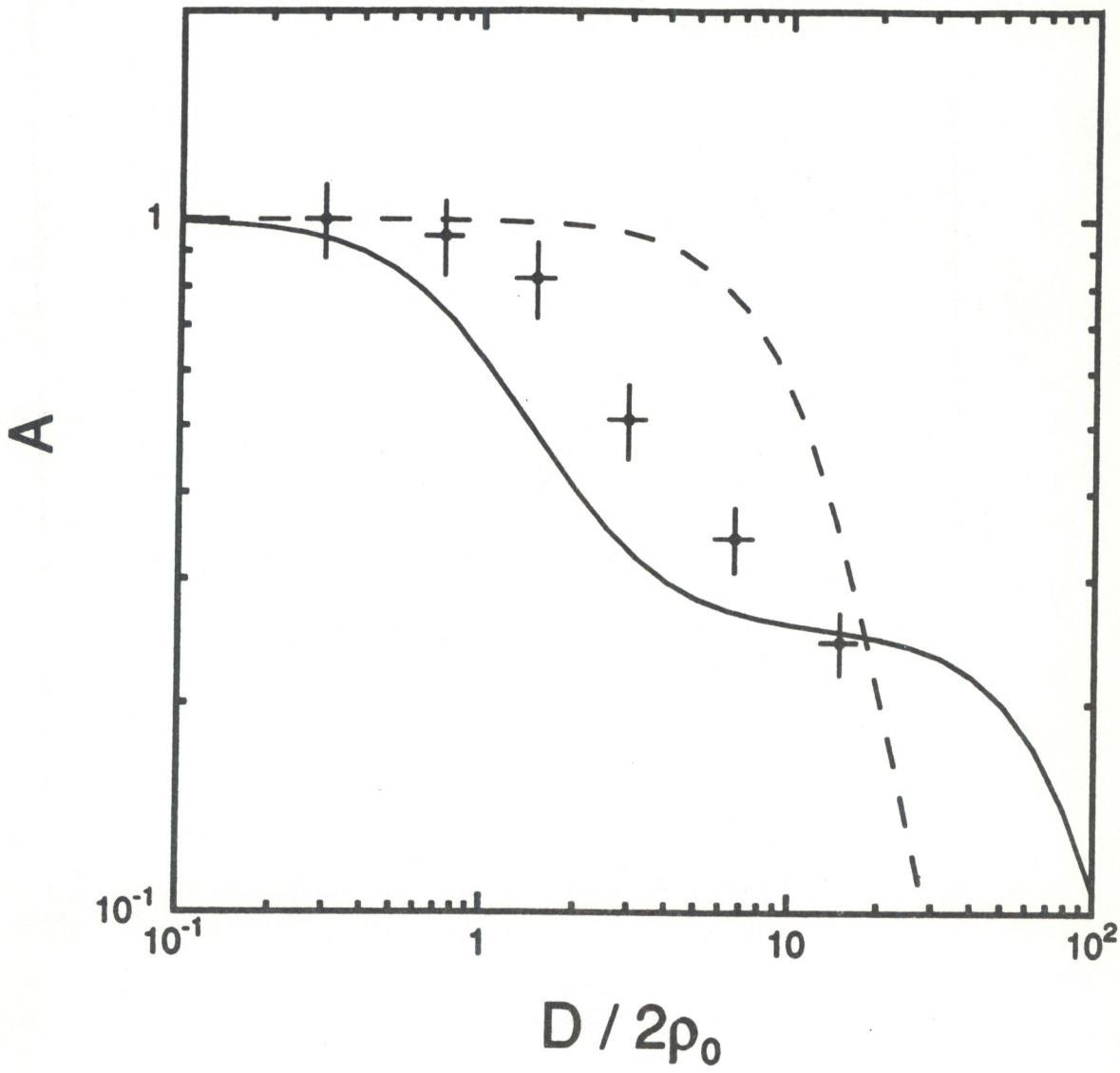

Figure 15. Aperture-averaging factor A vs. ratio of aperture radius $D/2$ to coherence length ϱ_0. The points represent data taken an 1000 m, the solid curve is the strong-turbulence approximation, and the dashed curve is the weak-turbulence approximation.

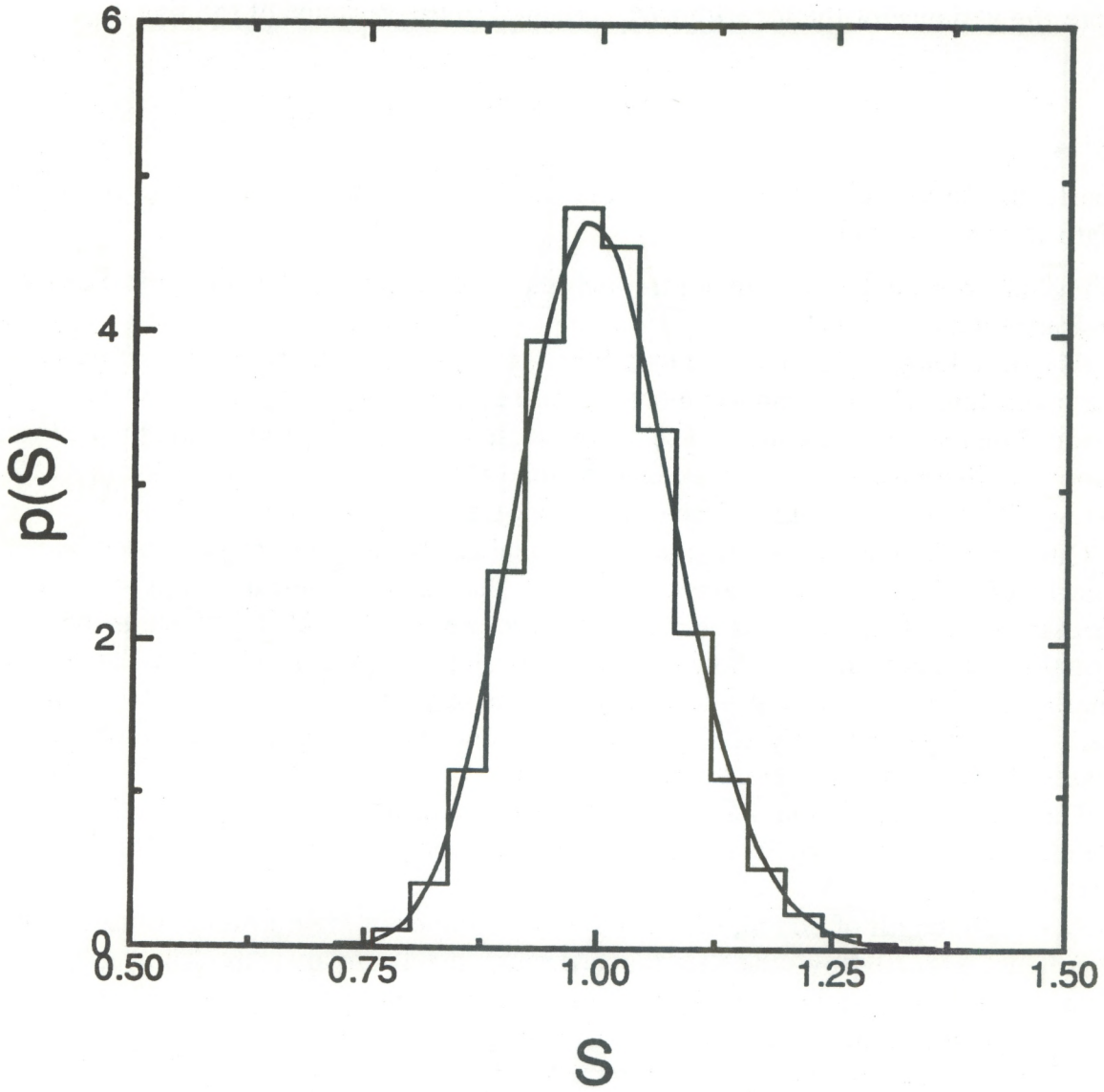

Figure 16. Plot of the probability density function *p* of the signal power *S* for data taken through a 1-mm-diameter aperture at a distance of 100 m. The stepped curve is a histogram of the data, and the smooth curve is a log-normal density function with the same variance.

formula is

$$p(S) = \frac{1}{\sqrt{2\pi}\ \sigma_{\ell n} S} \exp\left[-\frac{1}{2\sigma_{\ell n}^2}\left(\ell n\ S + \frac{1}{2}\sigma_{\ell n}^2\right)^2\right], \tag{91}$$

where the variance of the logarithm $\sigma_{\ell n}^2$ is related to the variance of the signal by

$$\sigma_S^2 = \exp\ (\sigma_{\ell n}^2) - 1\ . \tag{92}$$

Clearly, the data in Fig. 16 are log normal. In fact, all the data taken at the 100-m path length were log normal.

Fig. 17 presents the data taken through the 5-cm aperture, which is typical of the larger-aperture data.

At a path length of 250 m, the data begin to deviate slightly from log normal. The data taken through the 1-mm-diameter aperture, presented in Fig. 18, show the most deviation. The most notable difference is the height of the peak probability; the histogram is about 13% above the value predicted by the log normal. The variance for this case was 6.81×10^{-2}, and we should still be in the weak-turbulence regime.

Qualitatively, the deviations from log normal are the same as those caused by nonstationarity of turbulence as explained in Ref. 28. The standard deviation of the variance for this case was 66% of the mean value. Therefore, we conclude that deviations from log normal for this case are probably caused by nonstationarity of turbulence. For comparison, the standard deviation of the variance of the case of Fig. 16, which was much more nearly log normal, was only 20% of the mean value. As the aperture diameter was increased, the data became more nearly log normal.

The best fit was obtained for the 5-cm aperture; these data are presented in Fig. 19. The effects of nonstationarity can still be seen, but they have been partially mitigated by aperture averaging.

At a path length of 500 m, the data are deviating from log normal because of saturation effects. Fig. 20 shows the data taken through the 1-mm aperture. The variance for this case was 0.644, and some effects of saturation are expected. Differences between the data and the log normal, though not terribly large, are clear in the figure. As the aperture diameter increases, the data become more log normal.

Fig. 21 shows the data taken through the 5-cm-diameter aperture; these data are much more nearly log normal.

At the 1-km path length, the deviation from log normal is significant, but still not extreme. Fig. 22 presents the data from the 1-mm aperture. The variance for this case was 3.15, and we are well out of the weak path-integrated turbulence regime. Despite this, the log-normal density function may still be a reasonable approximation for some applications. As before, larger apertures produce signals that are more nearly log normal.

Fig. 23 presents data taken through a 1-cm aperture. The improvement is clear, although the data are not purely log normal.

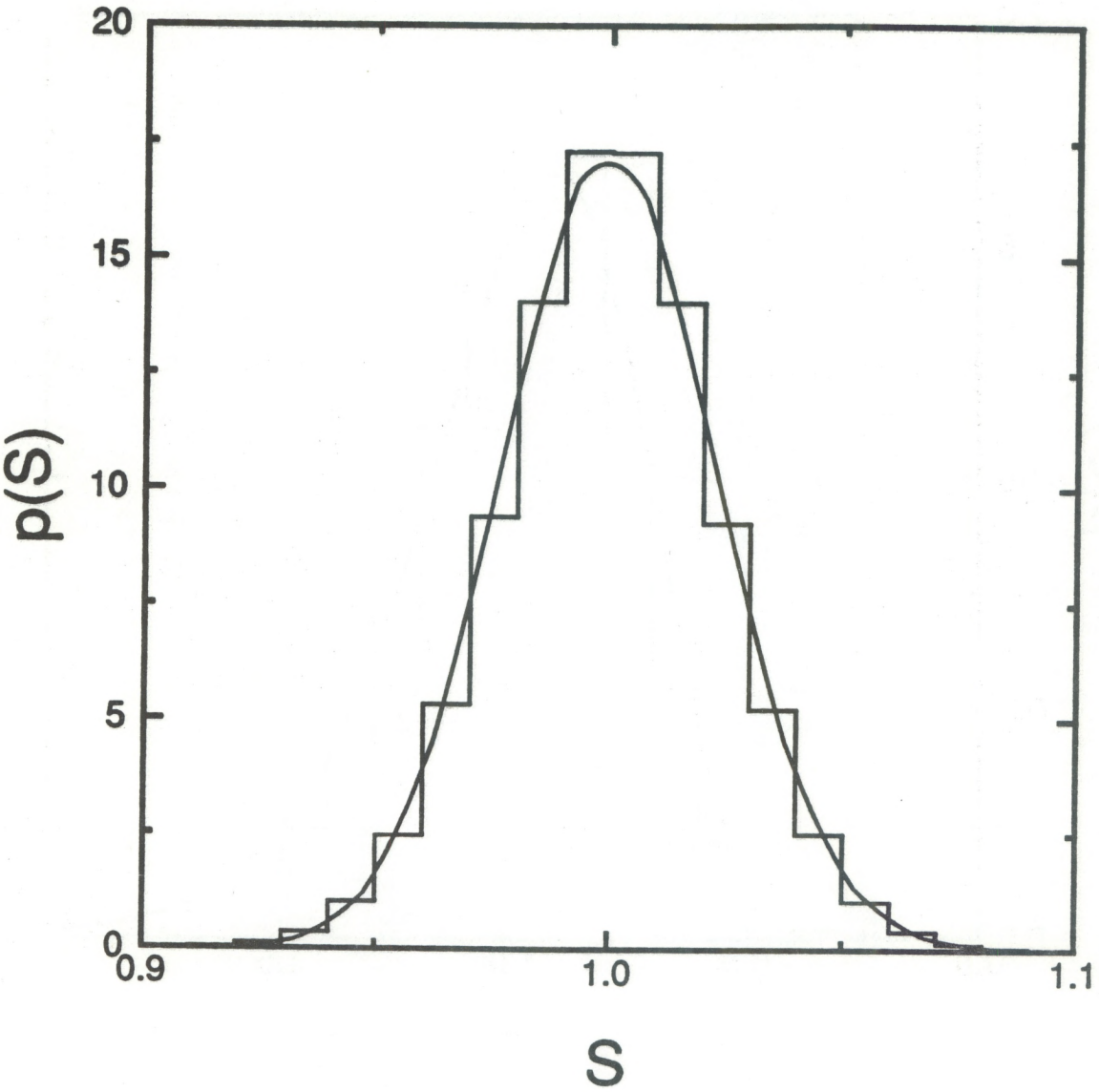

Figure 17. Plot of the probability density function p of the signal power S for data taken through a 5-cm-diameter aperture at a distance of 100 m. The stepped curve is a histogram of the data, and the smooth curve is a log-normal density function with the same variance.

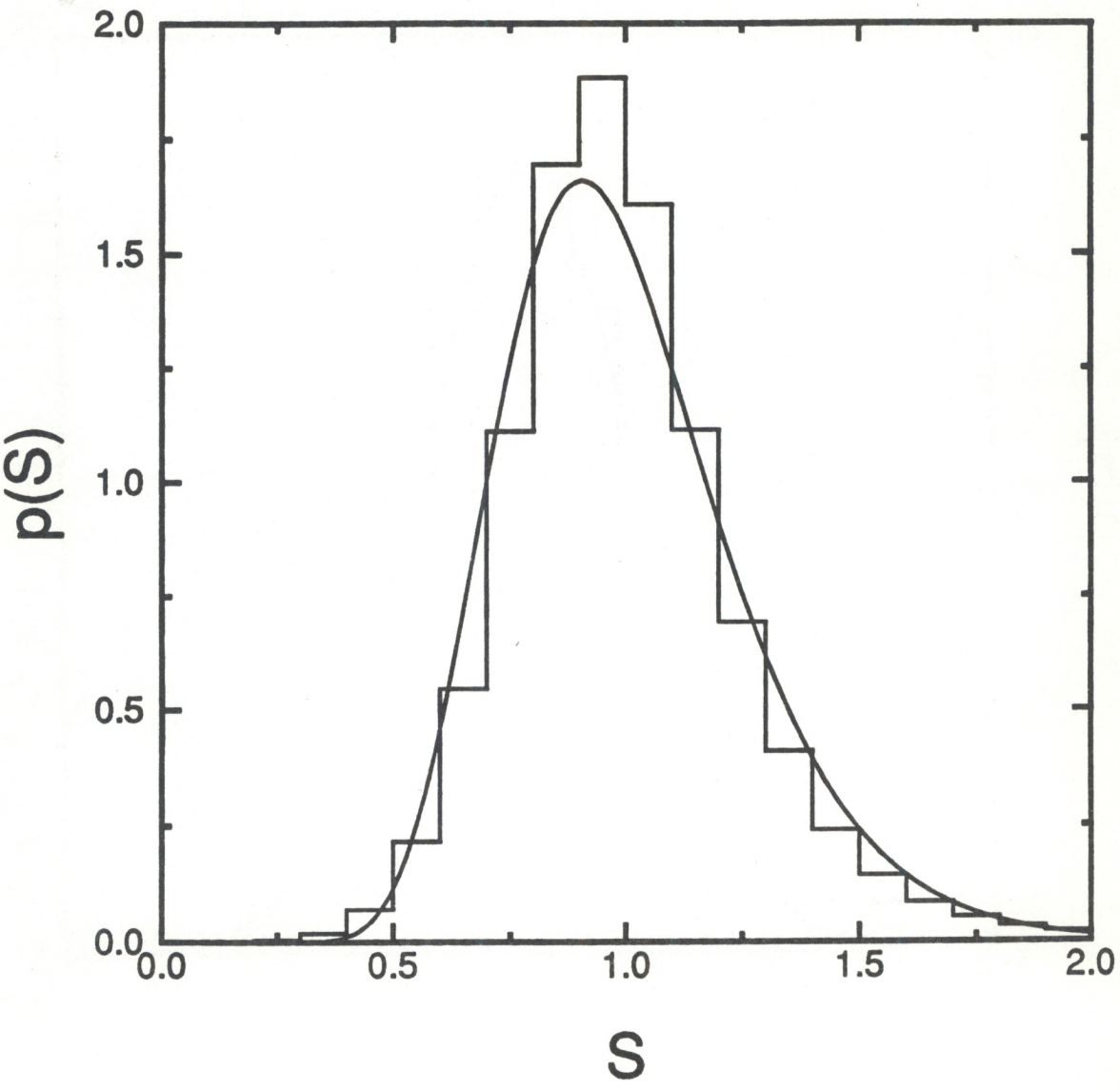

Figure 18. Plot of the probability density function p of the signal power S for data taken through a 1-mm-diameter aperture at a distance of 250 m. The stepped curve is a histogram of the data, and the smooth curve is a log-normal density function with the same variance.

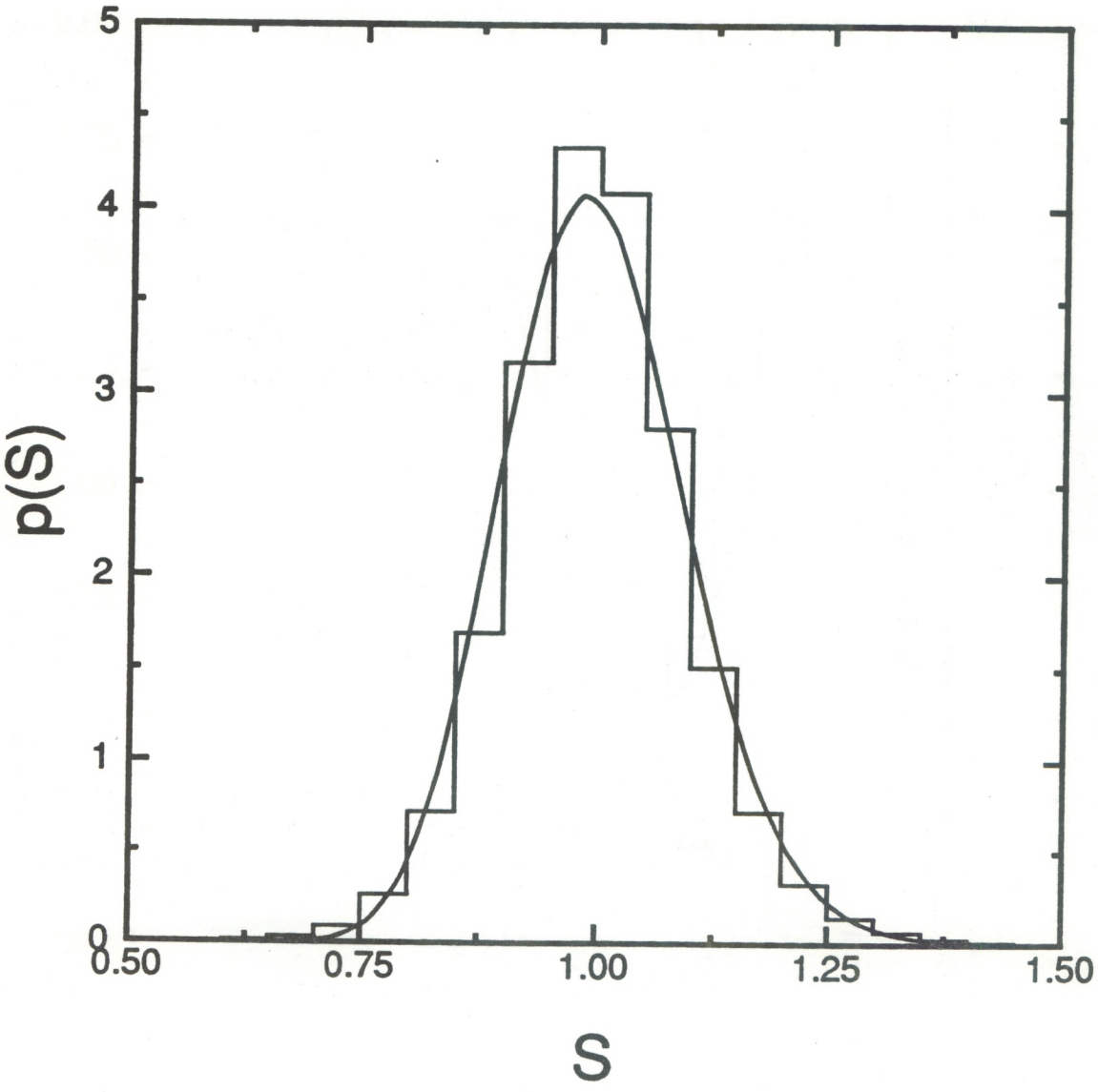

Figure 19. Plot of the probability density function *p* of the signal power *S* for data taken through a 5-cm-diameter aperture at a distance of 250 m. The stepped curve is a histogram of the data, and the smooth curve is a log-normal density function with the same variance.

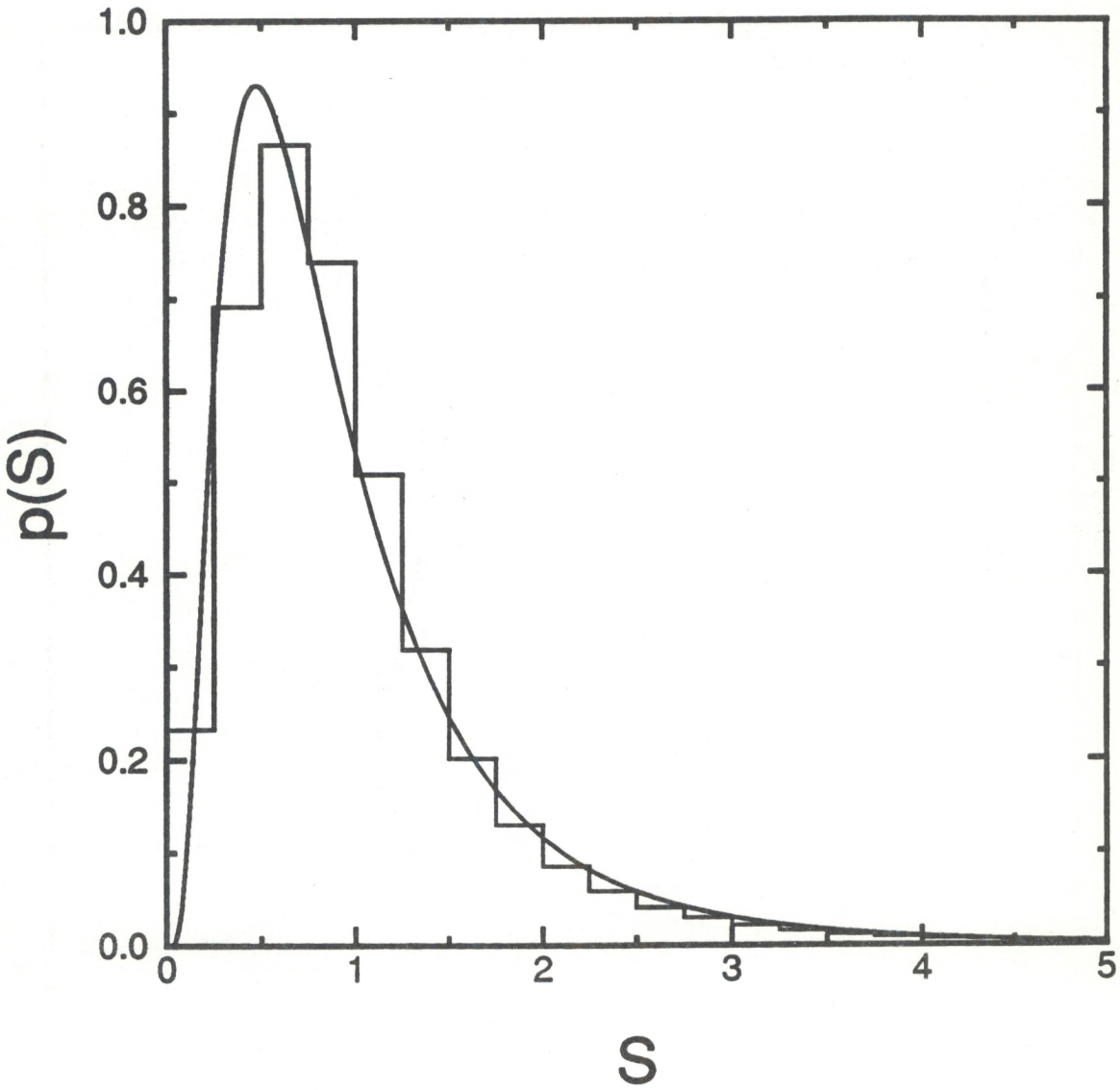

Figure 20. Plot of the probability density function *p* of the signal power *S* for data taken through a 1-cm-diameter aperture at a distance of 500 m. The stepped curve is a histogram of the data, and the smooth curve is a log-normal density function with the same variance.

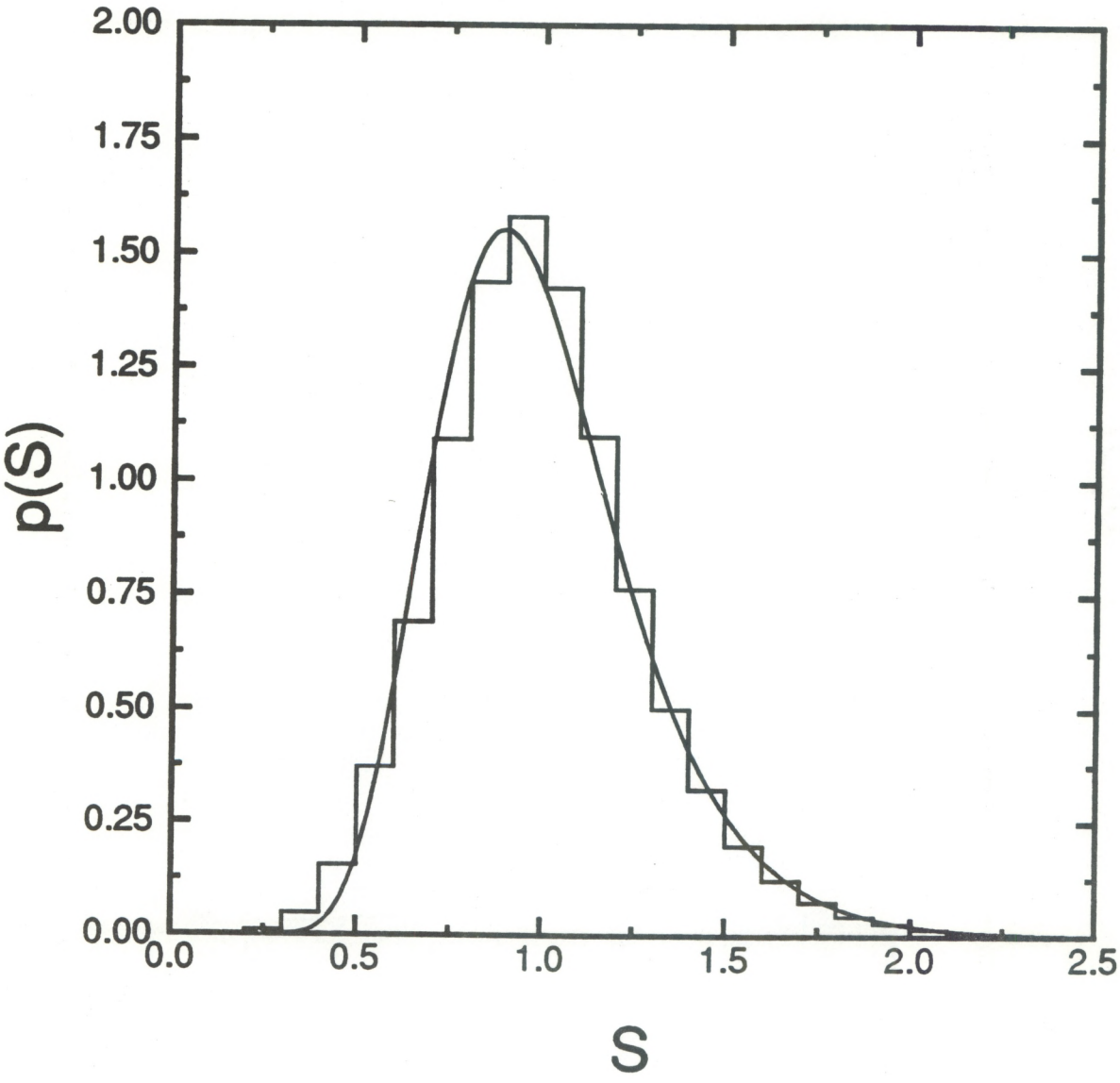

Figure 21. Plot of the probability density function *p* of the signal power *S* for data taken through a 5-cm-diameter aperture at a distance of 500 m. The stepped curve is a histogram of the data, and the smooth curve is a log-normal density function with the same variance.

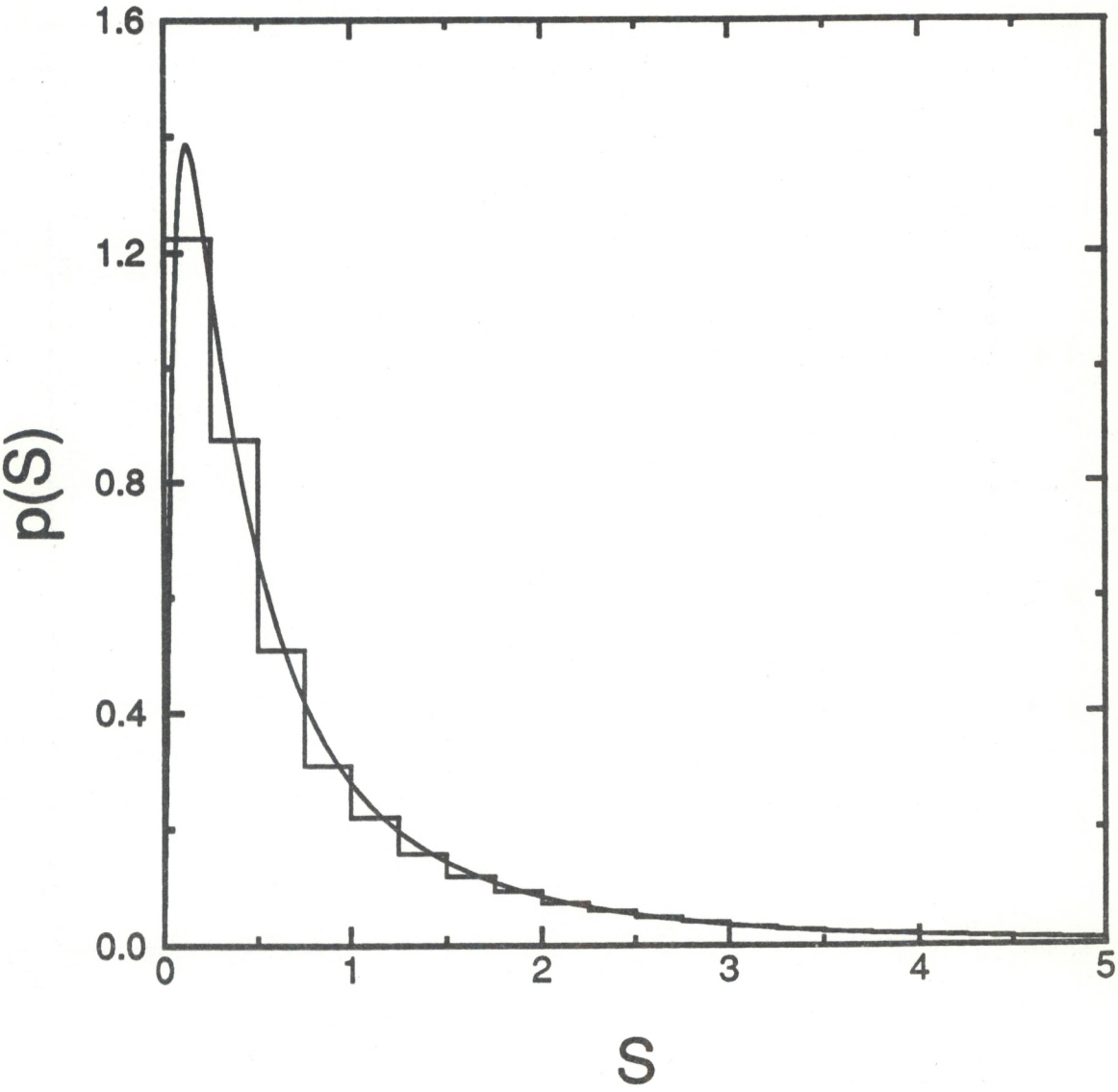

Figure 22. Plot of the probability density function *p* of the signal power *S* for data taken through a 1-mm-diameter aperture at a distance of 1 km. The stepped curve is a histogram of the data, and the smooth curve is a log-normal density function with the same variance.

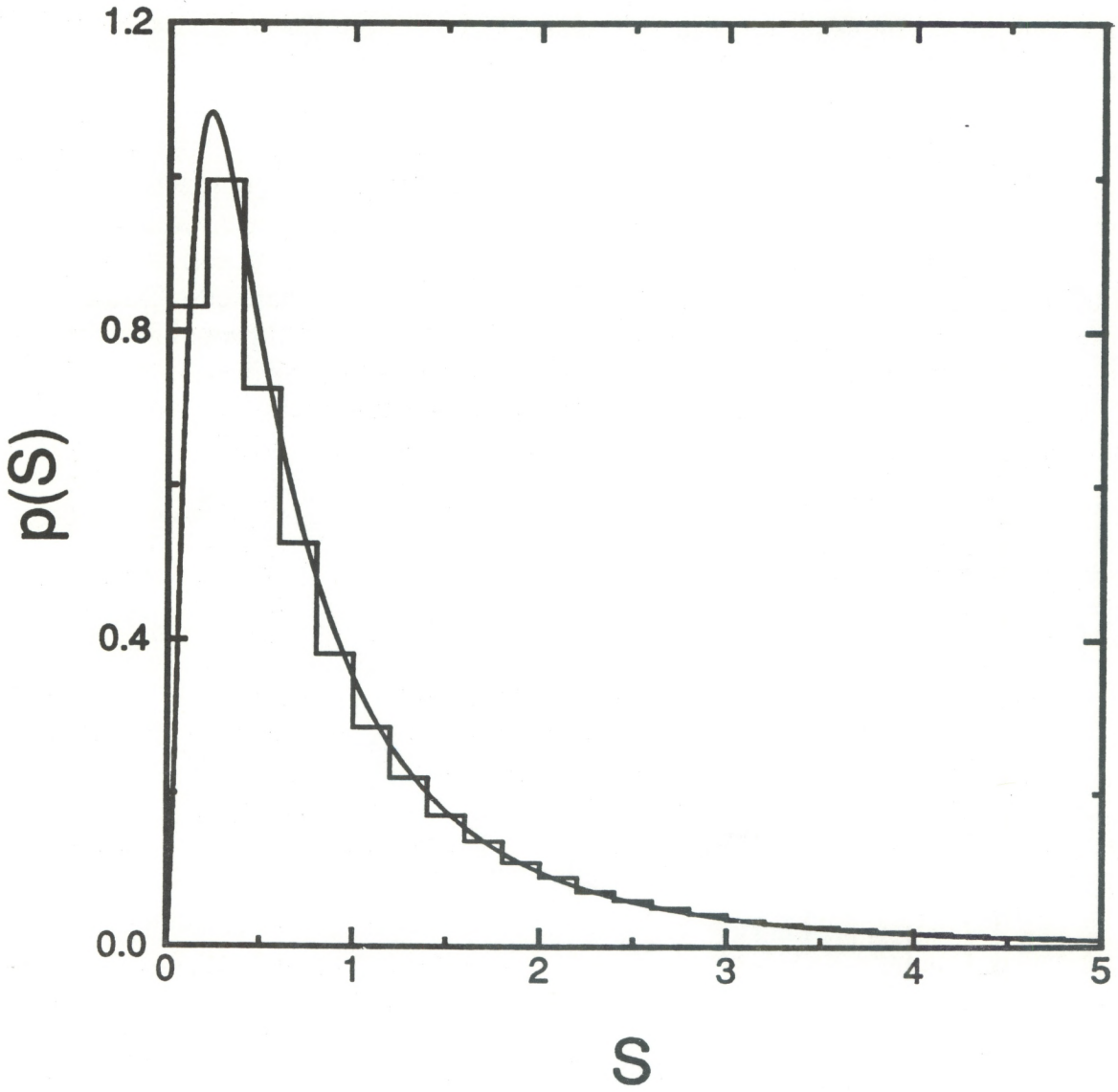

Figure 23. Plot of the probability density function *p* of the signal power *S* for data taken through a 1-cm-diameter aperture at a distance of 1 km. The stepped curve is a histogram of the data, and the smooth curve is a log-normal density function with the same variance.

Density function data at higher values of path-integrated turbulence are presented and compared with the log-normal density function in Ref. 29. These data are not repeated here. However, based on both data sets, we conclude that the log-normal probability density function is valid in stationary, weak turbulence and in strong turbulence for apertures larger than about three times the phase coherence length ϱ_0. Under other conditions, the log-normal density function is not as good, although it may be a sufficient approximation in many cases. The worst agreement is at small signal levels for small apertures in strong turbulence.

5. CONCLUSIONS

Approximate expressions have been found for the aperture-averaging factor in weak and strong path-integrated turbulence. These simple approximations are within about a factor of two of exact calculations and of experimental values under all conditions that could be investigated. The recommended approximations are summarized in Table 1 (plane-wave case) and Table 2 (spherical-wave case). The log-normal probability density function is found to be a reasonable approximation in a wide variety of circumstances.

ACKNOWLEDGMENTS

This work was partially supported by the U. S. Army Atmospheric Sciences Laboratory under Military Interdepartmental Purchase Request ASL 87–8013. Raymond Harrison wrote the software.

Table 1. Aperture-averaging factor for plane waves

Conditions	Formula
$\varrho_0 \geq (L/k)^{1/2}$ $\ell_0 \leq 2.73\ (L/k)^{1/2}$	$A = \left[1 + 1.07\left(\frac{kD^2}{4L}\right)^{7/6}\right]^{-1}$
$\varrho_0 \geq (L/k)^{1/2}$ $\ell_0 > 2.73\ (L/k)^{1/2}$	$A = \left[1 + 2.21\left(\frac{D}{\ell_o}\right)^{7/3}\right]^{-1}$
$\varrho_0 < (L/k)^{1/2}$ $\ell_0 \leq \varrho_0$	$A = \frac{\sigma_I^2 + 1}{2\sigma_I^2}\left[1 + 0.908\left(\frac{D}{2\varrho_o}\right)^2\right]^{-1}$ $+ \frac{\sigma_I^2 - 1}{2\sigma_I^2}\left[1 + 0.162\left(\frac{k\varrho_0 D}{2L}\right)^{7/3}\right]^{-1}$ $\varrho_0 = (1.46\ k^2\ L\ C_n^2)^{-3/5}$ $\sigma_I^2 = 1 + 1.22\left(\frac{k\varrho_0^2}{L}\right)^{1/3}$
$\varrho_0 < (L/k)^{1/2}$ $\ell_0 > \varrho_0$	$A = \frac{\sigma_I^2 + 1}{2\sigma_I^2}\left[1 + \left(\frac{D}{2\varrho_0}\right)^2\right]^{-1}$ $+ \frac{\sigma_I^2 - 1}{2\sigma_I^2}\left[1 + 1.27\left(\frac{k\varrho_0 D}{2L}\right)^{7/3}\right]^{-1}$ $\varrho_0 = (1.20\ k^2\ L\ C_n^2\ L\ \ell_0^{-1/3})^{-1/2}$ $\sigma_I^2 = 1 + 1.21\left(\frac{k\varrho_0\ell_0}{L}\right)^{1/3}$

Table 2. Aperture-averaging factor for spherical waves

Conditions	Formula
$\varrho_0 \geq (L/k)^{1/2}$ $\ell_0 \leq 1.5\ (L/k)^{1/2}$	$A = \left[1 + 0.214\left(\frac{kD^2}{4L}\right)^{7/6}\right]^{-1}$
$\varrho_0 \geq (L/k)^{1/2}$ $\ell_0 > 1.5\ (L/k)^{1/2}$	$A = \left[1 + 0.109\left(\frac{D}{\ell_o}\right)^{7/3}\right]^{-1}$
$\varrho_0 < (L/k)^{1/2}$ $\ell_0 \leq \varrho_0$	$A = \frac{\sigma_I^2 + 1}{2\sigma_I^2}\left[1 + 0.908\left(\frac{D}{2\varrho_o}\right)^2\right]^{-1}$ $+ \frac{\sigma_I^2 - 1}{2\sigma_I^2}\left[1 + 0.613\left(\frac{kD\varrho_0}{2L}\right)^{7/3}\right]^{-1}$ $\varrho_0 = (0.545\ k^2\ L\ C_n^2)^{-3/5}$ $\sigma_I^2 = 1 + 3.86\left(\frac{k\varrho_0^2}{L}\right)^{1/3}$
$\varrho_0 < (L/k)^{1/2}$ $\ell_0 > \varrho_0$	$A = \frac{\sigma_I^2 + 1}{2\sigma_I^2}\left[1 + \left(\frac{D}{2\varrho_0}\right)^2\right]^{-1}$ $+ \frac{\sigma_I^2 - 1}{2\sigma_I^2}\left[1 + 0.534\left(\frac{kD\varrho_0}{2L}\right)^{7/3}\right]^{-1}$ $\varrho_0 = (0.545\ k^2\ L\ C_n^2\ L\ \ell_0^{-1/3})^{-1/2}$ $\sigma_I^2 = 1 + 2.27\left(\frac{k\varrho_0\ell_0}{L}\right)^{1/3}$

REFERENCES

1. D. L. Fried, "Aperture Averaging of Scintillation," J. Opt. Soc. Am. *57*, 169–175 (1967).
2. V. I. Tatarskii, *Wave Propagation in a Turbulent Medium* (McGraw–Hill, New York, 1961), Chap. 13.
3. M. E. Gracheva and A. S. Gurvich, "Averaging Effect of the Receiving Aperture on Fluctuations in Light Intensity," Izv. V.U.Z. Radiofiz. *12*, 253–255 (1969).
4. R. F. Lutomirski, R. E. Huschke, W. C. Meecham, and H. T. Yura, "Degradation of Laser Systems by Atmospheric Turbulence," Report #R–1171–ARPA/RC, Rand Corporation, Santa Monica, California, June 1973.
5. A. G. Kjelaas and P. E. Nordal, "Scintillation Noise Reduction by Aperture Averaging in a Long-Path Laser Absorption Spectrometer," Appl. Opt. *21*, 2481–2488 (1982).
6. D. L. Fried, "Theoretical Analysis of Aperture Averaging," Report #DR–015, Optical Science Consultants, Yorba Linda, California, October 1973.
7. A. I. Kon, "Averaging of Spherical-Wave Fluctuations over a Receiving Aperture," Izv. V.U.Z. Radiofiz. *12*, 149–152 (1969).
8. R. F. Lutomirski and H. T. Yura, "Aperture-Averaging Factor of a Fluctuating Light Signal," J. Opt. Soc. Am. *59*, 1247–1248 (1969).
9. H. T. Yura and W. G. McKinley, "Aperture Averaging of Scintillation for Space-to-Ground Optical Communication Applications," Appl. Opt. *22*, 1608–1609 (1983).
10. S. J. Wang, Y. Baykal, and M. A. Plonus, "Receiver-Aperture Averaging Effects for the Intensity Fluctuation of a Beam Wave in the Turbulent Atmosphere," J. Opt. Soc. Am. *73*, 831–837 (1983).
11. D. H. Höhn, "Effects of Atmospheric Turbulence on the Transmission of a Laser Beam at 6328 Å. I. Distribution of Intensity," Appl. Opt. *5*, 1427–1431 (1966).
12. D. L. Fried, G. E. Meyers, and M. P. Keister, "Measurements of Laser-Beam Scintillation in the Atmosphere," J. Opt. Soc. Am. *57*, 787–797 (1967).
13. G. E. Homstad, J. W. Strohbehn, R. H. Berger, and J. M. Heneghan," "Aperture-Averaging Effects for Weak Scintillations," J. Opt. Soc. Am. *64*, 162–165 (1974).
14. R. S. Iyer and J. L. Bufton, "Aperture Averaging Effects in Stellar Scintillation," Opt. Commun. *22*, 377–381 (1977).
15. J. R. Kerr, "Experiments on Turbulence Characteristics and Multiwavelength Scintillation Phenomena," J. Opt. Soc. Am. *62*, 1040–1049 (1972).
16. R. S. Lawrence and J. W. Strohbehn, "A Survey of Clear-Air Propagation Effects Relevant to Optical Communications," Proc. IEEE *58*, 1523–1545 (1970).
17. R. J. Hill, "Models of the Scalar Spectrum for Turbulent Advection," J. Fluid Mech. *88*, 541–562 (1978).

18. R. J. Hill and S. F. Clifford, "Modified Spectrum of Atmospheric Temperature Fluctuations and its Application to Optical Propagation," J. Opt. Soc. Am. *68*, 892–899 (1978).

19. J. H. Churnside, "A Spectrum of Refractive Turbulence in the Turbulent Atmosphere," J. Mod. Opt. *37*, 13–16 (1990).

20. K. S. Gochelashvily and V. I. Shishov, "Multiple Scattering of Light in a Turbulent Medium," Opti. Acta *18*, 767–777 (1971).

21. K. S. Gochelashvily, V. G. Pevgov, and V. I. Shishov, "Saturation of Fluctuations of the Intensity of Laser Radiation at Large Distances in a Turbulent Atmosphere (Fraunhofer Zone of Transmitter)," Sov. J. Quant. Electron. *4*, 632–637 (1974).

22. A. M. Prokhorov, F. V. Bunkin, K. S. Gochelashvily, and V. I. Shishov, "Laser Irradiance Propagation in Turbulent Media," Proc. IEEE *63*, 790–810 (1975).

23. R. L. Fante, "Inner-Scale Size Effect on the Scintillations of Light in the Turbulent Atmosphere," J. Opt. Soc. Am. *73*, 277–281 (1983).

24. R. G. Frehlich, "Intensity Covariance of a Point Source in a Random Medium with a Kolmogorov Spectrum and an Inner Scale of Turbulence," J. Opt. Soc. Am. A *4*, 360–366 (1987)

25. M. Abramowitz and I. A. Stegun, eds., *Handbook of Mathematical Functions* (Dover, New York, 1970), Ch. 6, Ch. 13.

26. G. R. Ochs, W. D. Cartwright, and D. D. Russell, "Optical C_n^2 Instrument Model II," NOAA Tech. Memo. ERL WPL–51 (available from National Technical Information Service, 5285 Port Royal Rd., Springfield, VA, 22161; order number WPL51:PB 80–209000), 1979.

27. G. R. Ochs and R. J. Hill, "Optical-Scintillation Method of Measuring Turbulence Inner Scale," Appl. Opt. *24*, 2430–2432 (1979).

28. J. H. Churnside and R. G. Frehlich, "Experimental Evaluation of Log-Normally Modulated Rician and IK Models of Optical Scintillation in the Atmosphere," J. Opt. Soc. Am. A *6*, 1760–1766 (1989).

29. J. H. Churnside and R. J. Hill, "Probability Density of Irradiance Scintillations for Strong Path-Integrated Refractive Turbulence," J. Opt. Soc. Am. A *4*, 727–733 (1987).

☆U.S. GOVERNMENT PRINTING OFFICE: 1990 - 573-002/21021